NON-THROMBOGENIC SILK FIBROIN/N,N'-METHYLENE-DI-ACRYLAMIDE BLENDED SCAFFOLDS

A THESIS SUBMITTED TO THE GRADUATED SCHOOL OF APPLIED SCIENCES

OF

NEAR EAST UNIVERSITY

By

SAFWAN MOHAMMAD ALI

IN PARTIAL FULFILLMENT OF THE REQUIERMENTS FOR THE DEGREE OF MASTER OF SCIENCE

in

BIOMEDICAL ENGINEERING

LEFKOŞA 2013

CHAPTER 1 INTRODUCTION

1.1 Silk Fibroin

Silk fibroin is a natural polymer that has been used for medical and tissue engineering applications because of its biocompatibility and high tensile strength. Naturally it is coated with sericin a gum-like protein, which has to be detached for purification. Sericin protein works as glue that is intended to maintain the cocoon's structure [1]. However, for using silk as a biomaterial, sericin causes an opposing immune response if implanted [2].

1.2 Properties of Silk Fibroin

1.2.1 Chemical Properties of Silk Fibroin

Fibroin is an insoluble protein created by spiders, the larvae of *Bombyx mori*, and many other insects. Silk in its raw state comprises two main proteins, sericin and fibroin. Fibroin is the structural center of the silk, and sericin is the sticky material that surrounds it [3].

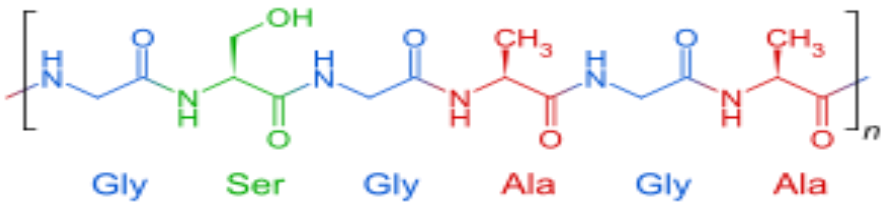

Figure 1.1 Primary structure of fibroin, [Gly-Ser-Gly-Ala-Gly-Ala] n [4]

The fiber is made up of two cores of fibroin concealed with a layer of sericin [1]. Silk fibroin consists of a light and heavy chain (25 kilo Dalton (kDa) and 350 kDa), that are connected together by a disulfide bond [5]. Generally, silk fibroin is a negatively charged protein at a neutral pH and has an isoelectric pH of about 3.8 [6]. The protein's random coil formation change to a β-sheet formation by the hydrophobic interactions, the β-sheet structure is the one responsible for the protein's outstanding tensile strength [7]. The fibroin protein is made of layers of antiparallel beta sheets. Its basic structure mainly contains the recurrent amino acid sequence $[Gly\text{-}Ser\text{-}Gly\text{-}Ala\text{-}Gly\text{-}Ala]_n$ where n is the number of the repeating sequence. The high glycine and alanine components permits tight packing of the sheets, which leads to the silk's

rigid structure that cannot be stretched (tensile strength). A blend of toughness and stiffness make it a material with applications in numerous areas, including biomedicine and textile manufacturing.

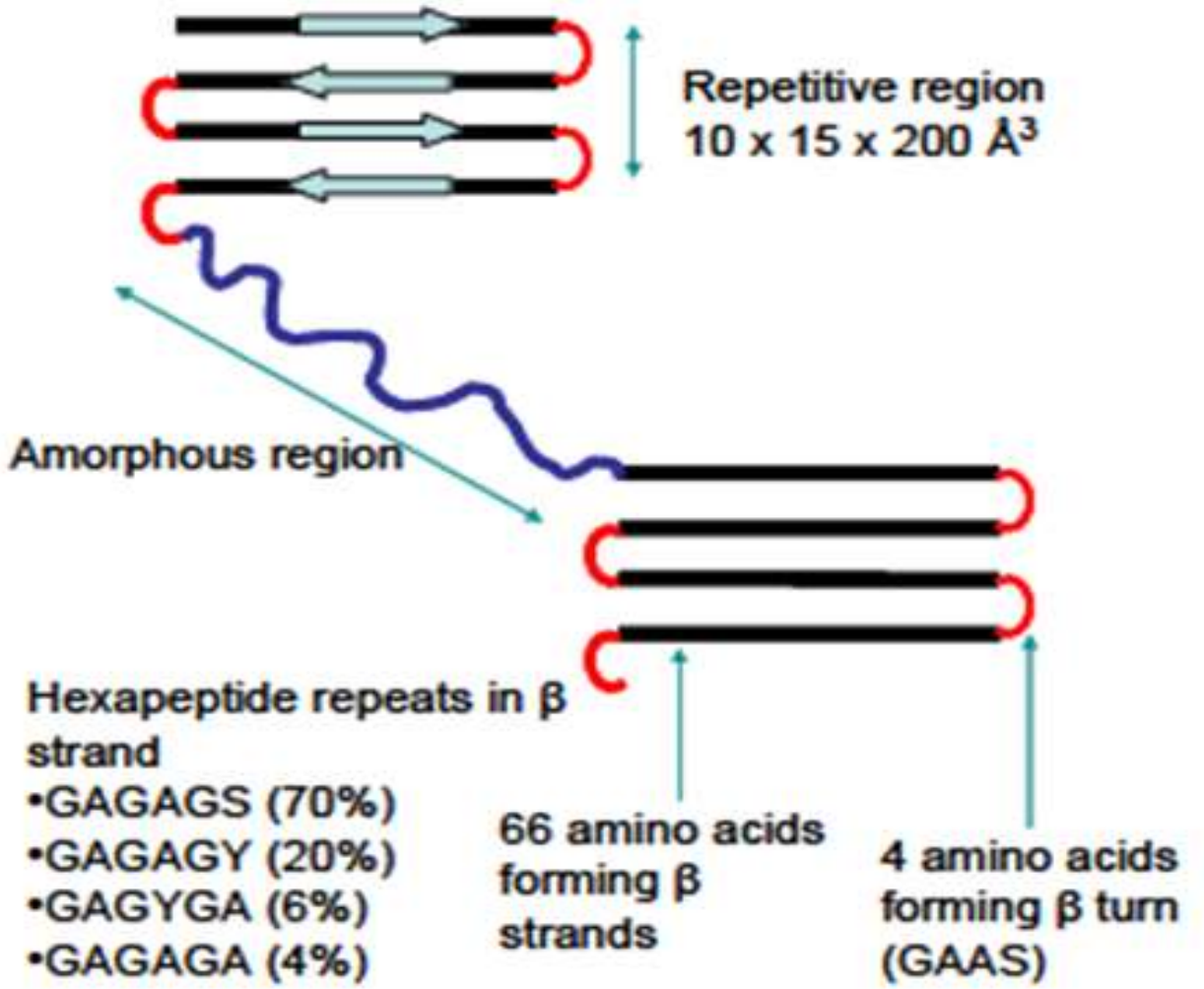

Figure 1.2 The schematic structure of *Bombyx mori* silk fibroin protein. The basic structure consists of 12 repetitive regions interspaced by 11 nonrepetitive regions. The repetitive region is responsible for the formation of β-sheets crystals of size 10x15x200 $Å^3$. The nonrepetitive region forms the amorphous part of the protein.

1 Å $=10^{-10}$ meters

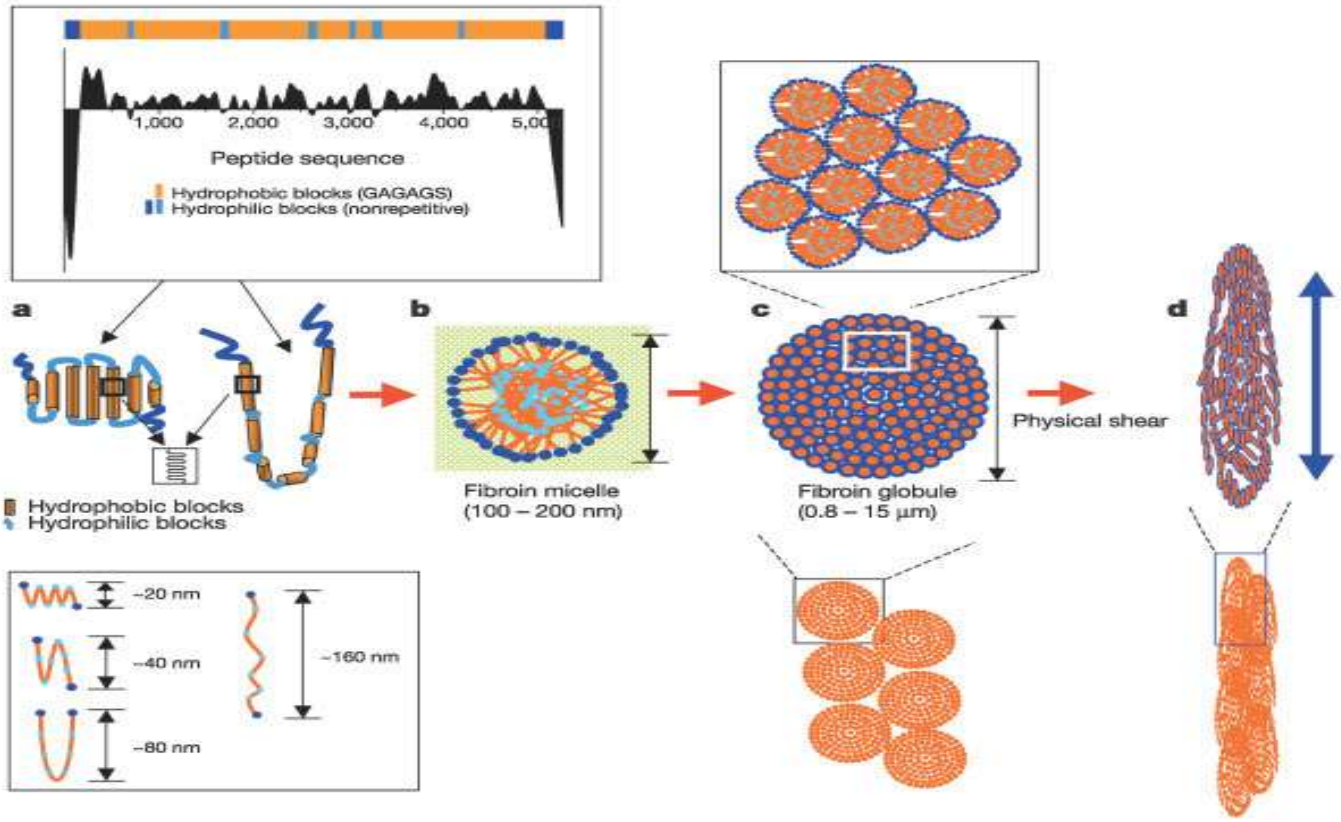

Figure1.3 Hydrophilic and hydrophobic regions, micelles, globules, fibrillar structures**a**, Hydrophobicity pattern in *B. mori* silk fibroin heavy chain primary sequence with possible chain folding intra- and inter-molecular schemes. **b**, Micelle assembly of silk fibroin in water (8%), based on hydrophilic–hydrophobic multiblock co-polymer structure leaving internal smaller hydrophilic domains to promote solubility in water, with larger-chain terminal hydrophilic blocks in contact with the surrounding aqueous solution. **c**, 'Globule' formation driven by increased fibroin concentration and lower water content, further hydrophobic interactions, and at the final stages by the presence of sericin or PEO. **d**, Elongation and alignment of globules and interactions among globules promoted by physical shear, leading to fibrillar structure [8].

Fibroin is known to be able to arrange itself in three structures, namely silk I, II, and III. Silk I is the natural form of fibroin, as produced from the *Bombyx mori* silk glands. Silk II is the organization of silk fibroin molecules in spun silk, which has higher strength and is usually used in several commercial applications. Silk III is a structure of fibroin which has been recently

discovered. Silk III is formed basically in solutions of silk fibroin at an interface (like. water-oil interface, air-water interface, etc.) [4].

1.2.2 Mechanical Properties

Silk is a very versatile biomaterial with its significant crystallinity, high elasticity, strength and toughness, and resistance to failure under compression. The combination of the β-sheet crystals, the interphase between the crystals, the semi-crystalline regions and the shear alignment of the molecular chains are the basis for silk's unique mechanical properties. While the highly organized β-sheet regions of the protein provide the tensile integrity, the semi-crystalline regions are the basis for the protein's elasticity [9]. The β-sheet structure affects the tensile properties, degradation rate and elasticity of the scaffold, so the tailoring of these properties can be done in part with the cross-linking process. The transition depends on the length of time exposed to the solvent as well as the solvent concentration. Methanol treatment is a widely used process to induce β-sheet formation although it does not transform all molecular regions. Ethanol, 1-Ethyl-3-[3-dimethylaminopropyl] carbodiimide [10] hydrochloride (EDC), glutaraldehyde or genipin also causes the transition from random coils to β-sheet configurations [1, 12, 13, and 14]. Studies show that regenerated silk fibers can hold their initial tensile integrity for 21 days within *in vitro* culture conditions [15]. Moreover, the solvent used for electrospinning can affect the β-sheet formation of the scaffold's secondary structure, which in turn can alter the mechanical properties. Formic acid, HFIP and water have been used to electrospin silk scaffolds, and of those, water and formic acid seem to enhance the mechanical properties of the scaffolds [16, 17].

1.2.3 Degradation

According to the US Pharmacopia, an absorbable biomaterial loses most of its tensile strength 60 days after implantation. Even though silk is considered non-degradable by this definition, it does in fact degrade but over a longer period of time. Silk will lose most of its tensile strength within a year *in vivo*, and will be unrecognizable at the implantation site within 2 years. However, the rate of degradation depends on the animal and the tissue implantation site. Silk is considered biodegradable because it is vulnerable to bacterial and enzymatic degradation. Studies show that proteases will cleave the protein at the less-crystalline regions after which the resulting peptides can be phagocytized by the cell [9, 11]. The solvent used to electrospin the silk scaffold may affect the degradation of the scaffold *in vivo* and *in vitro*. It was studied that

electrospinning from an aqueous solution instead of an organic solvent like HFIP can increase the degradation rate while promoting cell proliferation and penetration. The silk scaffold electrospun from an aqueous solution degraded between 2 and 6 months while those electrospun out of HFIP lasted over a year. Also methanol treatment can significantly decrease the degradation rate [11, 18]. There is a wide variety of biocompatible polymers used for tissue applications aside from silk fibroin. However, the degradation rates of other polymers cannot be tailored within such a high range as that of silk. Collagen, which is a widely used biomaterial, degrades between 1 to 4 weeks and sometimes longer depending on the cross-linking process [19]. Polycaprolactone (PCL) can last within the body for more than 2 years [20]. Another synthetic polymer, poly (lactic-co-glycolic acid) (PLGA) (85:15) usually degrades within 26 weeks, while PLGA (50:50) degrades between 6 and 8 weeks *in vitro* [21, 22, 23]. Silk scaffolds, however, can be modified to have similar degradation rates by changing the solvent for electrospinning [18].

1.2.4 Swelling properties

The degree of swelling depends on the ionization of the network, its degree of crosslinking and its hydrophilic/ hydrophobic balance [24] Changes in polymer compositions can influence the degree of swelling [25]. This can potentially increase the cumulative amount and rate of drug release. The swelling ratio of SF scaffolds has also decreased with an increase in Silk Fibroin concentration. Blending of Silk Fibroin with other materials such as chitosan [26, 27] and Hyaluronic acid [28] led to increase the swelling when compared with pure Silk Fibroin.

1.2.5 Solubility

Crystalline SF is insoluble in most solvents as well as in water, commonly applied to dissolve SF are highly concentrated salt solutions of lithium bromide, lithium thiocyanate calcium thiocyanate or calcium chloride [29]. These electrolyte solutions are able to disrupt the hydrogen bonds that stabilize β-sheets [30]. The possibility to control the solubility of SF not only allows for longer storage times for SF solutions but also for an increase in SF concentration without aggregation.

1.2.6 Biocompatibility

The foreign body response after the implantation of silk fibroin *in vivo* has been shown to be comparable to or even less than the other biomaterials in use today [9, 31, 32]. All-aqueous- and hexafluoroisopropanol (HFIP)-derived scaffolds have been tested in a one-year implantation study in rats. Those scaffolds were accepted by the host animals and the host immune response to the implanted scaffolds was low and local [33] this matches another study with SF films [29].

1.2.7 Thrombogenicity

Silk fibroin, which is the silk filament's core, is very attractive for biomedical applications as a protein-polymer. It can be processed into a diversity of 2-D and 3-D formats to match structural and morphological features of specific applications. This research was to associate the structure of silk fibroin with platelet activation in addition to inflammatory cell (THP-1 cell line) activation and adhesion, plasma protein adsorption. The amino-acid composition influenced the surface roughness of the films, crystallinity, biological interactions and hydrophobicity. Protein adsorption is minor on samples with the greater hydrophobicity and crystallinity, specifically the chemotactic factors (C3a, C5a and C3b); however other proteins like fibrinogen were similar in terms of adsorption. As a result, immune cells and platelets reacted in a different way to the numerous films acquired by following various processing procedures and stabilized by different methods (water vapor or methanol) in terms of their secretion of inflammatory mediators by monocytes, adherence and activation. This shows that by changing the chemistry the bioactivity can be influenced, like changing the source of the silk protein, or by altering or changing the process used in the materials preparation to evaluate the biological responses [34]. Another study found out that silk films and fibers are very promising for tissue engineering scaffold applications due to their physical properties, mainly where high tensile forces or mechanical loads are applied or in cases where slow degradation is required. The main issue is biocompatibility for biomaterial scaffolds. The inflammatory response of raw silk fibers was studied along with silk fibroin's extracts in an *in vitro* system. The results show that silk fibers are highly immunologically inert in short and long-term culture with RAW 264.7 murine macrophage cells whereas significant TNF release was induced by insoluble fibroin particles. Macrophage activation was not induced by soluble sericin a protein which is extracted from natural silk fibers. Although macrophages were not activated by sericin itself, it confirmed an

increasing effect of bacterial lipopolysaccharide. The low inflammatory potential level of silk fibers makes them useful for future biomedical applications [35].

1.3 Forms of silk fibroin

1.3.1 Silk Fibroin Microspheres

The use of silk fibroin as a biomaterial has been developed recently for biomedical engineering approaches in several ways as drug carriers. The Water-oil emulsion solvent diffusion method, this method is a simple and fast method for preparing both noncrosslinked and genipin crosslinked SF microspheres. The crosslinked and non crosslinked SF microspheres show great potential to act as drug carriers. The SF microspheres are completely spherical in shape and smooth in surface which can act as drug carriers particularly for hydrophilic drug delivery [36]. Silk fibroin microparticles prepared by spray dryer method would be used for the biomaterials with skin affinity and it is superior to other matrix materials and it might be applied for immobilization of drugs [37]. Laminar jet break-up of an aqueous SF solution spheres, These spheres have great encapsulation efficiencies and sustained release kinetics it helps to preserve the bioactivity of the embedded growth factor, with a great sustained release profile. The applications of those spheres may range from the controlled delivery of labile (likely to change) drugs and protein therapeutics to their use as a platform for the delivery of growth factors for tissue repair [38].

1.3.2 Silk Fibroin Nanoparticles

Reverse Microemulsion method for the preparation of nanoscale sized silk fibroin particles which have the capacity to encapsulate fluorescent dyes, can slowly degrade and is very biocompatible which is used for molecular imaging and bioassaying [39]. Capillary-microdot technique SF-derived curcumin nanoparticles show greater effectiveness against breast cancer cells and are likely to treat *in vivo* breast's tumors by local, sustained and long-standing biodegradable therapeutic delivery system. Delivery of curcumin to breast cancer cells is their main application [40]. As for the desolvation technique the nanoparticles were non-toxic to the cells and showed normal cell cycle distribution without any visible signs of cell arrest. The In-vitro release of loaded VEGF in the nanoparticles showed a sustained release of over 3 weeks without an initial burst, SF nanoparticles have great biocompatibility and degradability, so they

are used as carriers to deliver drugs to the target cells for diagnostics and therapeutics [41]. Silk fibroin was conjugated with methoxypoly (ethylene glycol) derivatives to prepare silk nanoparticles. The sizes and shapes of SF nanoparticles observed were ranged about 150-400 nm in diameter and spherical morphology. UV/VIS spectrometry showed SF nanoparticles might be outer PEG and inner SF structure [42].

1.3.3 Silk Fibroin films

By spin-assisted layer-by-layer assembly and spin coating robust multilayer ultrathin films of silk fibroin were fabricated. These films had an ultimate tensile strength along with a high elastic modulus (after treatment with methanol). The toughness was far superior to that commonly seen in conventional polymer composites .These exceptional properties are proposed to be caused by the slow but sure improvement of the self-reinforcing microstructure of highly crystalline β-sheets. These silk fibroin films with exceptional mechanical strength have possible applications in synthetic coatings for artificial skin, biocompatible implants and microscale Biodevices [43].

In another study the film is altered by SO_2 gas plasma treatment or by a two-step procedure together with NH_3 gas plasma treatment and reaction with 1, 3-propane sultone in order To increase the blood compatibility of the silk fibroin (SF) film, by the method of thrombin time (TT) prothrombin time (PT) and the activated partial thromboplastin time (APTT) tests *In vitro* antithrombogenecity was determined. Because of surface sulfonation the antithrombogenecity of the films treated increased immensely. The results showed that sulfonated SF films have a potential use of for blood-contacting biomaterial [44]. The ability to immobilize bone morphogenetic protein BMP-2 molecule in certain matrices can be very advantageous bone tissue engineering. Little if any osteogenesis was exhibited when human bone marrow stromal cells were cultured on an unchanged silk fibroin film in the presence of osteogenic stimulants, however the same cells cultured on silk fibroin films decorated with BMP-2 differentiated into an osteoblastic lineage in the presence of osteogenic stimulants as measured by their considerably raised calcium deposition, higher transcript levels of collagen type I, alkaline phosphatase activity, bone sialoprotein, osteocalcin, osteopontin, cbfa1 and BMP-2. The results show that BMP-2 attached on silk biomaterial backgrounds maintains the biological function *in vitro* based on the stimulation of osteogenic markers in seeded bone marrow stromal cells [45]. For peripheral nerve repair Nerve conduits (NC) have to guide the developing axons and shield

the axonal cone from any harm. The NC must degrade after finishing its purpose to remove the need of consequent explanation and to enhance nerve regeneration it should be fitting for controlled drug release of some implanted growth factors. Silk fibroin (SF) is a slowly biodegradable and biocompatible biomaterial with outstanding mechanical properties that could meet the requirements stated previously. SF films supported the metabolic activity and adherence of PC12 cells and Supported neurite outgrowth during PC12 cell differentiation in combination with nerve growth factor (NGF). Further research must be done for the use of SF-NC for the assessment in peripheral nerve reparation and the growth factors delivery [46].

1.3.4 Silk fibroin electrospun nanofibers

For the use of tissue engineering electrospinning is a technique that fabricates nano-scale nonwoven materials. It combines a high voltage power source with a translating and spinning mandrel and a polymer of choice. Figure 4 illustrates a typical electrospinning setup with a grounded collector

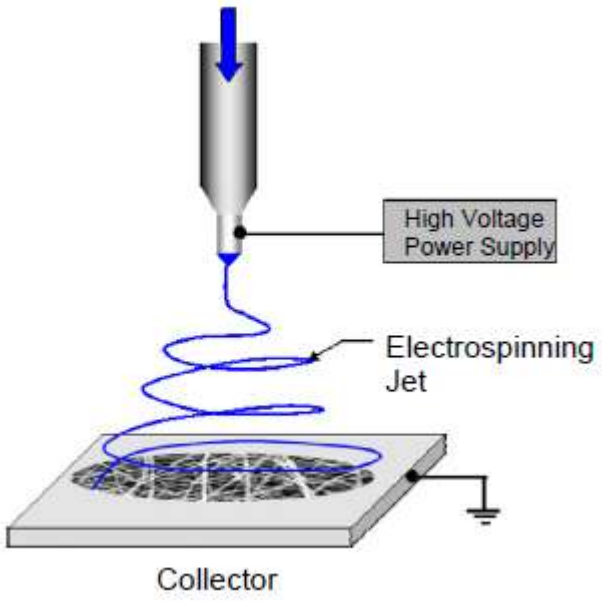

Figure 1.4 A typical electrospinning setup with a grounded collector [47].

By the electrostatic repulsion between the charges at the surface of the solution droplet along with the force generated by the electric field between the needle tip and the target, the fiber formed [48]. The numerous process parameters, such as voltage, flow rate, rotation, solution

concentration and air gap distance, can be manipulated to modify the scaffold's properties. The shape and size of the scaffold is determined by the shape and size of the mandrel used. A diversity of natural and synthetic polymers creates quality electrospun scaffolds for tissue engineering applications [49]. These polymers can be electrospun alone or blended together to alter the properties of the scaffold. The kind of polymer(s) and formulating conditions improved the, biocompatibility mechanical properties, degradation rate and porosity. For the electrospun silk fibroin scaffolds, by varying the viscosity , flow rate, solution concentration, air gap distance, electric field, type of solvent and the angle and diameter of the spinneret the fiber diameters are controlled [50]. Regenerated silk fibroin electrospins as a random coil structure, however the β-sheet formations is attained by treating the scaffold with a cross-linking agent or methanol [51].To form a novel silk-gauze combination for wound dressing, Silk Fibroin (SF) nanofibers were electrospun onto plasma-treated 100% cotton gauze bandages. Atmospheric pressure plasma pre- and post- treatments were used to raise the adhesion between the cotton substrates and SF nanofibers. Because of the presence of a nanofiber layer on the substrate Moisture vapor transport and Air permeability were considerably reduced. The results showed that the durability and adhesion increase are generally because of the active species caused by the plasma on the exterior surface of the cotton substrate as well as on the silk fibroin nanofibers surface [52].

1.3.5 Silk Fibroin gel

When the Silk fibroin is in a solution, when some conditions are altered can make a transition into a gel. If the temperature increases, the pH decreases or the concentration increases, the solution will gel because the silk fibroin molecules will go through a change from the random coil formation to a β-sheet formation. At a low pH and at high temperatures the regenerated silk fibroin solution becomes very unstable which will activate the transition. By altering the concentration of the regenerated silk fibroin solution the pore sizes and mechanical properties of the hydrogel can be controlled as well [53]. The transition can be initiated from the addition of calcium chloride with or without the combination of ethanol or water, the addition of methanol, ethanol or PEO, freeze drying, sonication, gas foaming or salt leaching [54-59]. The gel is a porous white cloudy gel that can endure compression. Due to its biocompatibility, porous structure and strength Silk fibroin gel can be used for various tissue engineering applications.

1.3.6 Silk Fibroin Scaffolds

It is also emerging in the field of tissue engineering as a material for tissue engineering anterior cruciate ligaments (ACL) as the matrix was built to match the natural human ACL Properties they found that SF can provide suitable biomaterial matrices to support adult stem cells differentiation toward ligament lineages along with its excellent mechanical properties and biocompatibility [60], using silk fibroin in conjugation with an inorganic compound as a material for bone tissue engineering The blend of gelatin/SF was used as a based protein scaffold which was used to initiate osteogenesis and showed great properties as porosity, good water absorption ability. However the biodegradability occurred in the protein part and the scaffold as a whole showed a low cytotoxicity level [61].By biomimetic synthesis a novel bone-like biomaterial of silk fibroin (SF) and hydroxyapatite (HAP) composite was developed. The SF/HAP composite then confirmed that it can stimulate new bone formation *in vivo* and osteoblast proliferation *in vitro*. This novel biomaterial is an encouraging material for bone regeneration and replacement [62]. Silk fibroin scaffolds were prepared from aqueous silk fibroin solutions by combining salt-leaching and freeze drying Methodologies. However the mechanical properties of the scaffold exhibited concentration dependence. The scaffold showed great stability and maintained its properties after *in vitro* degradation for 30 days. It also shows that it is suitable for meniscus and cartilage tissue engineering [63]. SF in conjugation with poly (3-hydroxybutyrate-co-3-hydroxyhexanoate) (PHBHHx) has been used to fabricate the tissue engineered cardiovascular scaffolds due to its controllable and suitable mechanical properties. However it was found that SF-modified PHBHHx scaffolds are highly biocompatible with cardiovascular-related cells, showing that it can be utilized for the extensive applications of PHBHHx in the cardiovascular regeneration [64]. In another study it is found that silk fibroin has good biocompatibility with rat dorsal root ganglia (DRG) and is also beneficial to the survival of Schwann cells without exerting any significant cytotoxic effects on their phenotype or functions, which can open a gateway for silk fibroin as a material for nerve tissue engineering [65]. Another study about a developed novel method for cross-linking a silk fibroin solution by gamma irradiation to form a hydrogel that might serve as a dermal scaffold. The silk fibroin hydrogel is not cytotoxic to human fibroblasts or human keratinocytes. The mechanical properties of the silk fibroin hydrogel formed by gamma irradiation method were superior to that of silk fibroin hydrogel created using a freeze-drying method. The silk fibroin hydrogel created using this novel method is suitable as a

dermal scaffold in skin tissue engineering [66]. Recently silk fibroin and elastin scaffolds were produced for the treatment of burn wounds SF & Elastin scaffolds were produced for the treatment of burn wounds. The excellent properties of SF were combined with elastin protein and resulted in a scaffold which mimics the extracellular matrix (ECM). By using genipin as a cross-linker they obtained scaffolds with smaller pore size and reduced swelling ratio degradation and release rates. The composition had a great effect on the scaffold's physical properties; composition can be easily controlled to make the scaffold suitable for biological applications. The cytocompatibility with human skin fibroblasts along with the healing improvements make these scaffolds suitable for wound dressing applications [67]. Silk fibroin has an exceptional and valuable blend of properties, including great biocompatibility and outstanding mechanical performance. These features provided key principles for the usefulness of scaffold/matrix made of regenerated silk fibroin for tissue engineering. The silk fibroin scaffolds utilized for the tissue engineering must degrade at a rate that matches the rate of growth of the tissue. The results confirm that a high content of β-sheet structure gives a low degradation rate in the scaffold. The results show that to in order to control and manipulate the degradation rate of the scaffold it is done by adjusting the content of β-sheet structure [68]. The preparation of SF for applications in tissue engineering was studied, Pure SF was extracted from silk worm cocoons by degumming and solubilizing and then further purification was carried out. However the results indicate that the regenerated silk fibroin can be used for fabrication of porous silk fibroin scaffolds for various tissue engineering applications [69]. For tissue engineering, it is very important to design and control the pore architecture of three-dimensional (3D) polymeric scaffolds, which plays an important role in directing tissue formation and function. Different pore structures were formed according to the pH of silk fibroin because silk fibroin exhibits water-like behavior under basic conditions and gel-like behavior under acidic conditions [70]. The pore architecture of scaffolds plays a critical role in tissue engineering as it provides the vital framework for seeded cells to organize into a functioning tissue. By manipulating the concentration the pore sizes of the scaffolds decreased as the concentration of fibroin protein increased. Human bone marrow mesenchymal stromal cells (BMSC) transfected with the BMP7 gene were cultured in different pore sized scaffolds. The results showed that BMSC expressing BMP7 preferred a pore size between 100 and 300 microns in silk fibroin protein fabricated scaffolds, with better cell proliferation and ECM production. Furthermore, *in vivo* transplantation of the silk fibroin

scaffolds combined with BMSC expressing BMP7 induced new bone formation. This means that optimized pore architecture of silk fibroin scaffolds can modulate the bioactivity of BMP7-transfected BMSC in bone formation [71].

1.4 Scaffolds and Cell Culturing

The design of new scaffolds mimicking the natural environment during tissue formation is an important issue in biomaterials research. Silk fibroin and hyaluronan scaffolds were prepared with porous microstructures by freeze-drying silk fibroin and hyaluronan aqueous solutions also to induce water insolubility of silk fibroin they were incubated in methanol. For three weeks Mesenchymal stem cells were seeded and cultured on silk fibroin/hyaluronan scaffolds. After cell culture, enhanced ingrowth of the cells into silk fibroin/hyaluronan scaffolds was shown by the histology of the constructs as compared to pure silk fibroin scaffolds. However Silk fibroin/hyaluronan scaffolds are good as a biomimetic platform for mesenchymal stem cells in the field of tissue engineering [72]. Scaffold composition, configuration and resulting properties critically affects tissue development. The influence of silk fibroin concentration and correspondent processing method (aqueous or HFIP-derived) and three-dimensional scaffold structure (lamellar or porous, with distinct pore size) on bone tissue formation by osteogenic differentiation of human adipose tissue derived stem cells (hASC) were studied. It was observed that very similar bone tissue was formed in all silk fibroin scaffold groups, evaluated by alkaline phosphatase activity, calcium production, collagen type I deposition and scaffold bone volume fraction [73]. Due to the high surface area of the fibers with nanoscaled diameters, biomaterial scaffolds are provided with a lot of benefits. A study was carried out concerning the adhesion, proliferation and spreading of human bone marrow stromal cells (BMSCs) on these matrices. Biocompatibility and biodegradability properties of the silk matrix along with the electrospun silk matrices ability of supporting BMSC attachment, spreading and growth *in vitro*, propose possible usage of these matrices as scaffolds for tissue engineering [74]. Before lyophilization, freezing temperature and NaCl concentration of the silk fibroin solution were varied in order to modify the morphology of the lyophilized silk fibroin 3D-scaffolds. Sponge-like interconnected porous networks resulted after freezing at -22°C, however, stacked leaflet structures formed after fast freezing at -73°C. The usage of millimolar NaCl (50-250mM) increased the porosity of the scaffolds. The seeding of P19 embryonic carcinoma cells showed that the presence of salt and freezing conditions influenced the cell distribution into the scaffolds, with salt addition

increasing the access of cells to deeper regions [75]. Pore architecture of scaffolds is known to play a critical role in tissue engineering as it provides the vital framework for the seeded cells to organize into a functioning tissue, in this study different concentrations and pore sizes were investigated, The pore size of the scaffold decreases as the concentration of fibroin protein increases, Human bone marrow mesenchymal stromal cells (BMSCs) transfected with BMP7 gene were cultured in these scaffolds, The results showed that BMP7 expressing BMSCs preferred a pore size between 100 and 300 μm of silk fibroin protein fabricated scaffolds, with better cell proliferation and ECM production , *in vivo* transplantation of the silk fibroin scaffolds combined with BMP7-expressing BMSCs induced new bone formation. This study identified that optimized pore architecture of silk fibroin scaffolds could modulate the bioactivities of BMP7 transfected BMSCs in bone formation [76]. Starting from a variety of cell sources including primary cell-based and stem cell based platforms cartilage tissue can be engineered. cellular responses of isolated human embryonic stem cells, human chondrocytes and mesenchymal stem cells (MSCs) derived out of these three sources adipose tissue, bone marrow and human embryonic stem cells, were used with two biomaterials chitosan and silk scaffolds, in the presence and lack of bone morphogenetic protein 6 (BMP6), well-preserved chondrogenic phenotype with unique characteristics in both scaffolds with regard to cartilage formation were shown by embryonic stem cells-derived MSCs, embryonic stem cells-derived MSCs were favorable for cartilage formation, especially in the silk scaffolds with BMP6. Results show that cell source differences are important for chondrogenic outcomes; however, human embryonic stem cells-derived MSCs were utmost favorable cell source [77]. In order to engineer bone-like tissue *in vitro*, human bone marrow derived mesenchymal stem cells (hMSCs) and porous biodegradable silk scaffolds were used. It is shown that RGD-silk scaffolds are mainly appropriate for cells from a patient's own body bone tissue engineering, because of their stable macroporous structure, mechanical properties which are identical to those of the natural bone, and slow degradation [78]. Increased calcium deposition and alkaline phosphatase activity was observed out of the differentiation of hMSCs for 3 and 5 weeks in spinner flasks in osteogenic cell culture medium when compared to control medium. The newly formed tissue pore structures and that the structure of the tissue-engineered bone was altered by controlling the underlying geometry of the scaffold [79]. Human bone marrow-derived mesenchymal stem cells (hMSCs) were sowed on collagen, silk, and crosslinked collagen scaffolds. On the silk fibroin scaffolds,

cells proliferated faster than on the collagen matrices. The silk was three times greater in terms of the total content of glycosaminoglycan deposition as compared to collagen scaffolds. Cartilage-like tissue was distributed homogeneously throughout the whole silk scaffolds; angular or round-shaped cells existed in deep gaps in the silk systems. These results propose that silk fibroin scaffolds are proper for cells from patients own body cartilage tissue engineering in serum-free medium and enable mechanical improvements along with compositional features suitable for long-term implants to generate or regenerate cartilage [80].

1.5 Blood coagulation

1.5.1. Activated partial thromboplastin time (APTT)

The activated partial thromboplastin time (aPTT or APTT) or partial thromboplastin time (PTT) is an indicator evaluating the efficiency of both the common coagulation pathway and the "intrinsic" which is now called the contact activation pathway. Away from detecting blood clotting abnormalities [81] it is also used to screen heparin's treatment effects, which is an anticoagulant. However APTT is used in combination with the prothrombin time (PT) which determines the extrinsic pathway. The typical range of the PTT is between 30 seconds and 50 seconds. Some researches indicate that the shortening of the PTT might increase the risk of thromboembolism [82]. For normal PTT times, the presence of these coagulation factors is required: I, II, V, VIII, IX, X, XI, & XII. Especially, lacks in factors VII or XIII will not be noticed with the PTT test.

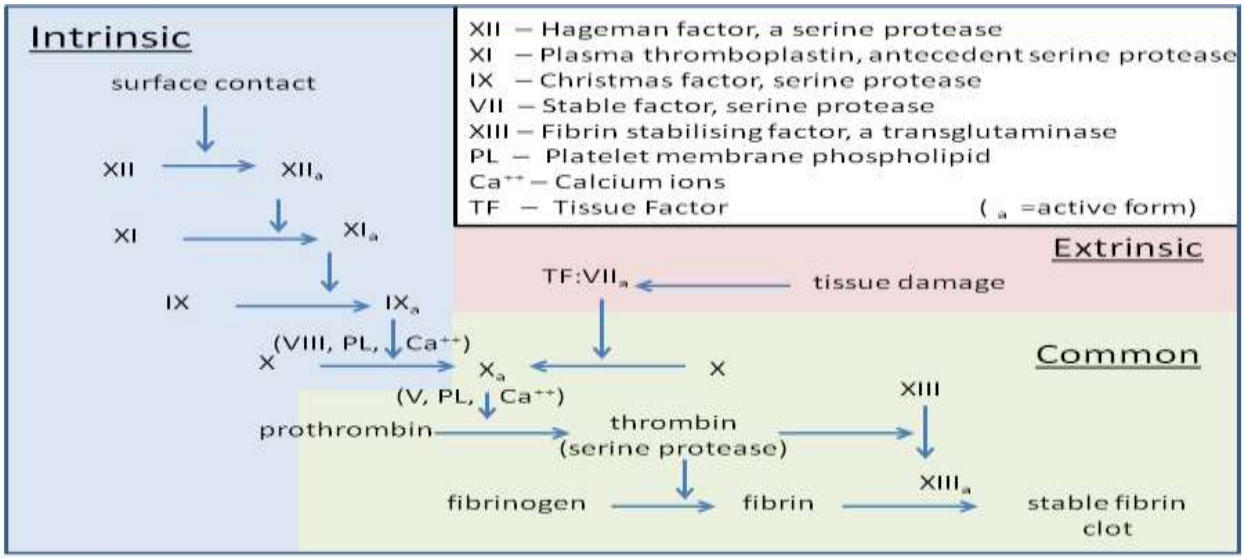

Figure 1.5 The three pathways that makeup the classical blood coagulation pathway [83]

1.5.2 Prothrombin Time

The prothrombin time (PT) and its derived measure international normalized ratio (INR) are measures of the extrinsic pathway of coagulation. This test is also called "ProTime INR" and "PT/INR". They are used to determine the blood's clotting tendency. PT measures factors I (fibrinogen), II (thrombin), V, VII, and X. That is classic extrinsic pathway. It is used in a combination with the activated partial thromboplastin time (aPTT) which measures the intrinsic pathway. The normal range for prothrombin time (PT) is generally around 12-16 seconds, and for the INR in the lack of anticoagulation therapy is usually 0.8-1.2.

1.6 Problem statement

The need for new biocompatible materials is rising as the world continues to progress in tissue engineering, checking the biocompatibility is crucial for *in vivo* applications. Therefore this research will focus on the *in vitro's* Thrombogenicity of the silk fibroin scaffolds and see its effect on the blood coagulation time to see the possibility of applying them on blood contacting surfaces.

CHAPTER 2 MATERIALS AND METHODS

2.0 Introduction

This chapter describes the general materials and experimental methods used in the synthesis and application methods of silk fibroin scaffolds.

2.1 Materials

Domesticated *Bombyx Mori.* Cocoons were used to obtain the pure silk fibroin after purification processes which are explained in (section 2.2.3); Na_2CO_3 (sigma-Aldrich) was used in the degumming step. Calcium chloride ($CaCl_{2)}$ also purchased from Sigma-Aldrich and used in the dissolution step along with 98% ethanol and ultra-pure water for the preparation of the electrolyte solution. Dialysis membrane (Sigma-Aldrich) (cut off M.W. 12,400), this tubing will retain most proteins of molecular weights of 12,000 or more, since the full average diameter of the dialysis membrane is 16 mm, average flat width 25 mm (1.0 in.) capacity of ~60 mL/ft. Methylene bisacrylamide $C_7H_{10}N_2O_2$ as a crosslinker for scaffold preparation.

Figure 2.1 Raw Silk cocoons

2.2 Methods

2.2.1 PBS Preparation

Table.1 Phosphate Buffer Saline Contents

Salt	**Concentration (mmol/L)**	**Concentration (g/L)**
NaCl	137	8.01
KCl	2.7	0.20
$Na_2HPO_4 \bullet 2\ H_2O$	10	1.78
KH_2PO_4	2.0	0.27
pH	7.4	7.4

After preparing the PBS solution the pH is adjusted to 7.4 by adding either hydrochloric acid (HCl) or sodium hydroxide (NaOH) depending on the pH value whether it's below or above 7.4

2.2.2 Acetic Acid Solution Preparation

Glacial acetic acid is diluted by water to get 0.5M acetic acid after that the pH is adjusted to 1.2 by HCl if the pH value goes beyond that point it can be reversed back by NaOH.

2.2.3 Silk Fibroin Purification

2.2.3.1 Degumming

Degumming is the process of removal and separation of the sericin protein (which acts as a glue) from the fiber structure (silk fibroin) protein. This procedure was carried out by placing a beaker containing silk cocoons in a 0.1M sodium carbonate ($Na_2CO_{3)}$ solution 1g/100ml (w/v) at 75°C on a hot plate stirrer at the speed of 1.5 rpm, through three sessions, half an hour each. Then the degummed silk was washed and rinsed thoroughly to get rid of the remaining solution and then they were dried overnight in the laboratory at room temperature to obtain the silk fibers.

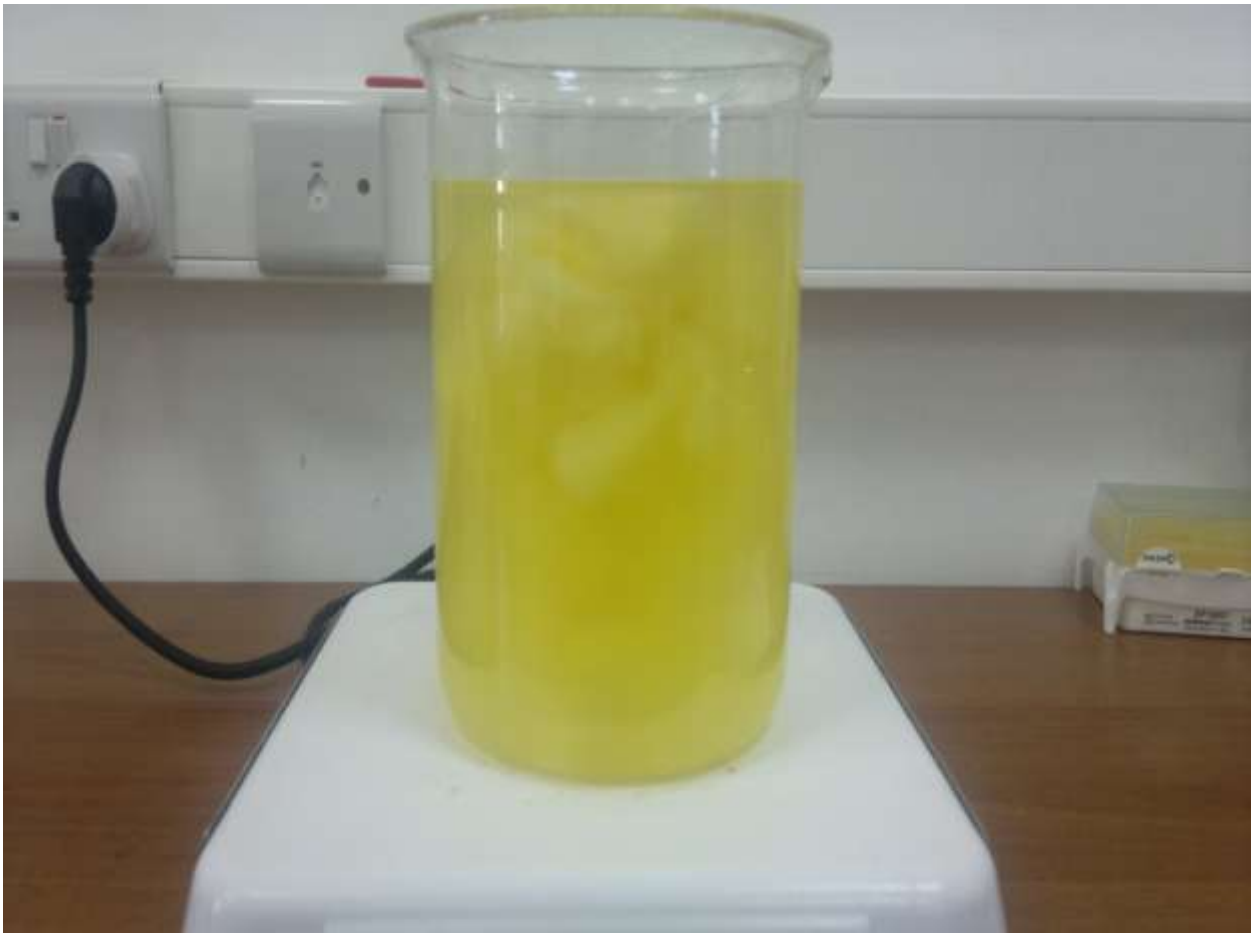

Figure2.2 Degumming process

Figure 2.3 Degummed Silk fibers

2.2.3.2 Dissolution

Dissolution is the process of dissolving the silk fibers to have an aqueous form of silk fibroin; the main principle is breaking down the long polypeptide chains into shorter chain lengths to get an aqueous silk fibroin solution. This is performed by mixing SF with ηC_2H_5OH:ηH_2O:$\eta CaCl_2$; (2:8:1) molar ratio at 75°C with continuous stirring until total dissolution. This results in an electrolyte solution with aqueous silk fibroin; however by altering the w/v (weight of the fibers to the electrolyte solution's volume) different aqueous Silk fibroin concentrations can be obtained.

Figure 2.4 Silk fibers dissolving in the electrolyte solution

Figure 2.5 Aqueous silk fibroin obtained from dissolution in semipermeable membranes

2.2.3.3 Dialysis

This step so far is concerned with the removal of the ions within the solution obtained from the dissolution step, however this is done by pouring the solution into a semipermeable membrane tube and placing the membrane into a large beaker (5 liters) filled with distilled water. This will allow the ions to diffuse from the silk/electrolyte solution through the membrane to the water. This procedure was repeated several times at different periods (1, 3, 6, 9, 12, 12 hours) with continuous stirring. This process ends up with the formation of a pure aqueous silk fibroin.

Figure 2.6 Dialysis of the aqueous silk fibroin against distilled water

Figure 2.7 Pure aqueous silk fibroin

2.2.4.1 Scaffold preparation and crosslinking

The aqueous Silk fibroin was placed into a 5ml syringe and mixed with crosslinkers with different proportions or kept pure as shown in Table.2, the syringe was then placed into a deep freezer at -20°C or -80°C initially for 3-4 hours and it is placed into a beaker filled with chilled ethanol at -20°C for 6-7 hours. The scaffold was removed and washed with PBS pH=7.4 and left to dry at room temperature.

Figure 2.8 Silk fibroin scaffold freezed in the syringe

Figure 2.9 Silk fibroin scaffolds

2.2.4.2 Thin scaffolds preparation

The aqueous silk fibroin was placed in a petri dish and left in the deep freezer for 3-4 hours and peeled of and placed into 80% chilled ethanol beaker for 6-7 hours. The thin scaffold was removed and washed with PBS pH =7.4 and left to dry at room temperature.

Figure 2.10 Thin scaffold

Figure 2.11 Thin scaffold

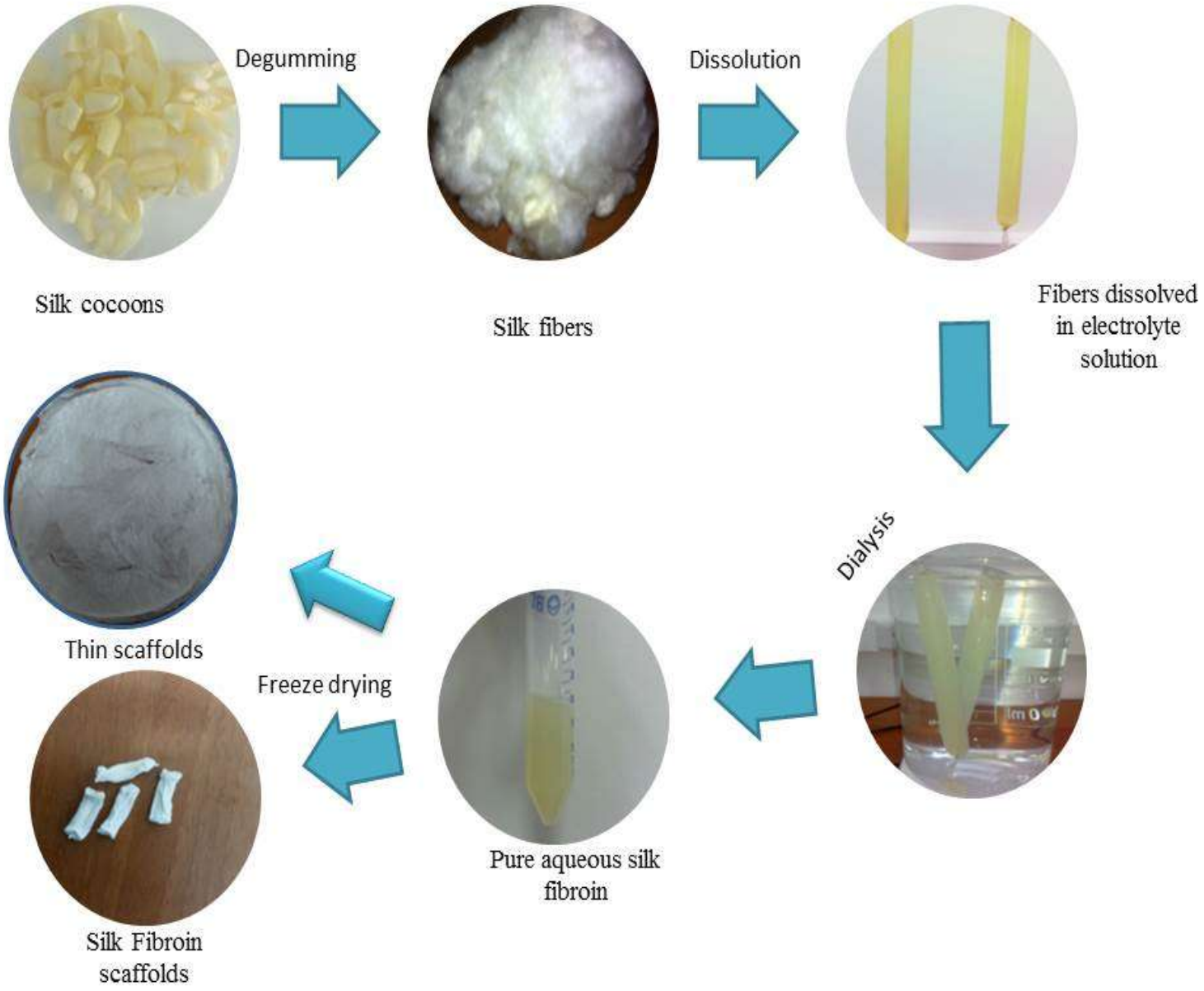

Figure 2.12 Silk purification diagram

2.2.5 Protein Concentration Calculation

For the sake of calculations, by taking 1 ml of the aqueous silk fibroin solution and placing it in a petri dish and applying heat (37°C) to it a film of the SF protein is formed, by weighing that film the exact protein content within 1 ml can be calculated since the water evaporates leaving a pure protein film.

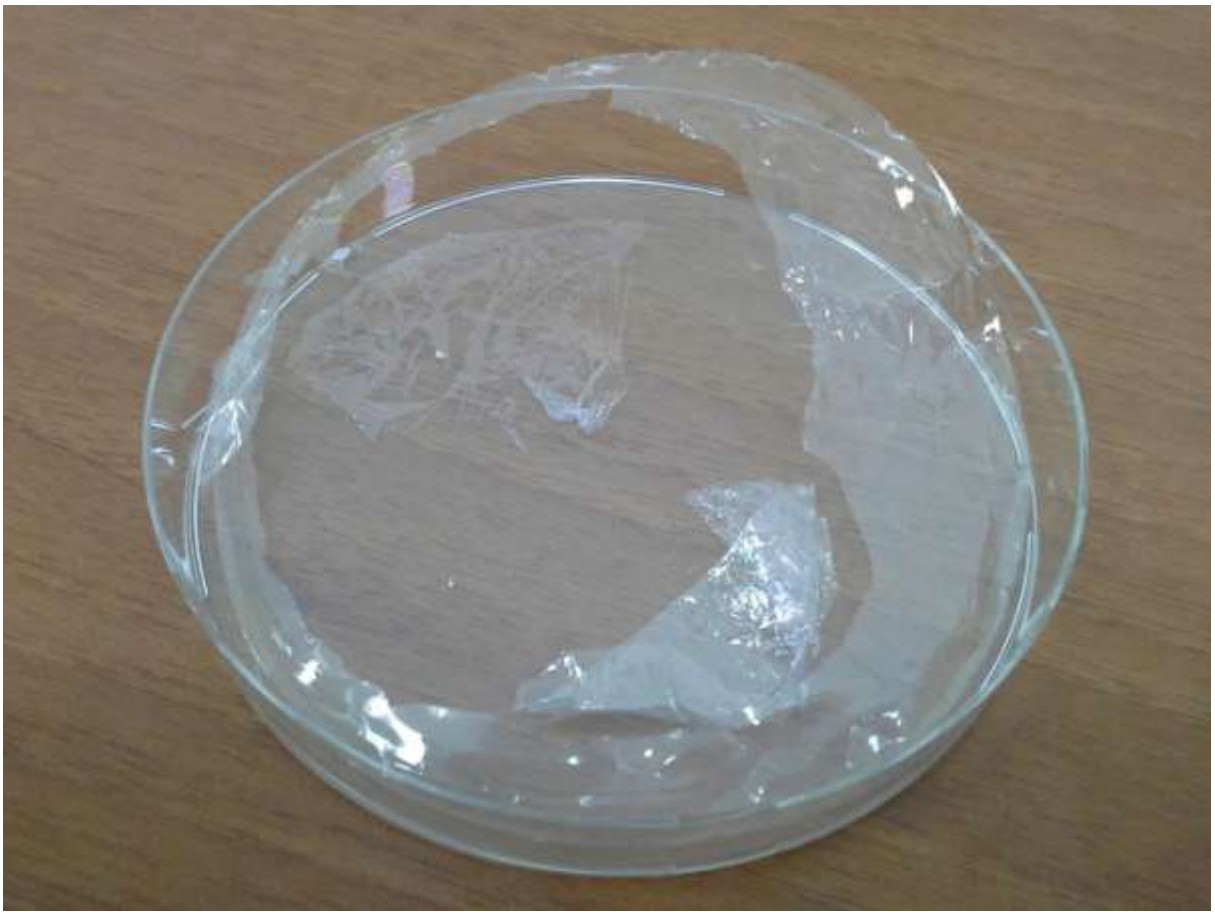

Figure 2.13 Silk fibroin film formed to obtain the protein's concentration

2.2.6 Silk Fibroin with Different Concentration and Crosslinking Proportions Preparation

The aqueous SF obtained was 4% w/v, 5% w/v and 6% w/v SF/ ($CaCl_2$:H_2O:C_2H_5OH) electrolyte solution. However for preparing those ratios it is necessary to note that the exact content of SF in the solution after dialysis decreased to half of the original intended, that's due to the water leakage into the aqueous silk fibroin solution, the 4%, 5%, and 6% solutions before dialysis became 2%, 2.5% and 3% all w/v after dialysis.

For the 6% aqueous silk fibroin the weight of the film was determined for 1 ml aqueous silk fibroin it contained 0.0297 g/ml. which is 2.97% w/v.

The scaffolds prepared were freeze dried in -20°C and -80°C for each concentration and for the 3% SF w/v it was mixed with methylene bisacrylamide $C_7H_{10}N_2O_2$ as a crosslinker, 3 samples with different proportions were prepared, these three proportions were prepared for both -80°C and -20°C for a total of 6 samples as shown in Table.2

2.2.7 Swelling

After the scaffolds were prepared with different proportions they were tested for their swelling properties in the PBS and ABS solutions.

The swelling ratios were calculated by using:

$$Swelling\ \% = \frac{\text{weight(t)} - \text{weight(dry)}}{\text{weight(dry)}} * 100\% \quad \text{..... Eq. (1)}$$

Where weight (t) is the scaffold's weight measured at any given time and the weight (dry) is the weight of the scaffold in its dry state.

2.2.8 Biodegradation

For the biodegradation test a solution of protease and water was used with 0.3 g/ml concentration and the scaffolds were tested against the protease solution at 37°C to match with the body's temperature.

The biodegradation percentage can be calculated by applying the equation:

$$Biodegradation\ (Weight\ loss)\% = \left(\frac{weight\ (t)}{initial\ weight}\right) * 100\ \% \quad \text{.....Eq. (2)}$$

Where weight (t) is the scaffold's weight measured at any time given and the initial weight is the weight of the scaffold taken after soaking it in the protease solution for 2 minutes and squeezing it.

2.2.9.1 Activated Partial Thromboplastin Time (APTT)

Human Blood samples were collected in tubes with citrate to bind the calcium therefore stopping the coagulation. The specimen is then taken to the laboratory to get the intrinsic pathway activated; calcium was added to inverse the anticoagulant effect of the oxalate and an activator are mixed into the plasma sample. The time is measured up to the point of a clot formation. This test is called partial because the reaction mixture is free of the tissue factor.

2.2.9.2 Prothrombin Time

The prothrombin time is measured using the blood's plasma. Blood is drawn into a test tube containing liquid citrate, by binding the calcium it acts as an anticoagulant. The blood is mixed and centrifuged to isolate the plasma from the blood cells [84]. Factor III (Tissue factor) is added and the time the sample takes to clot is measured.

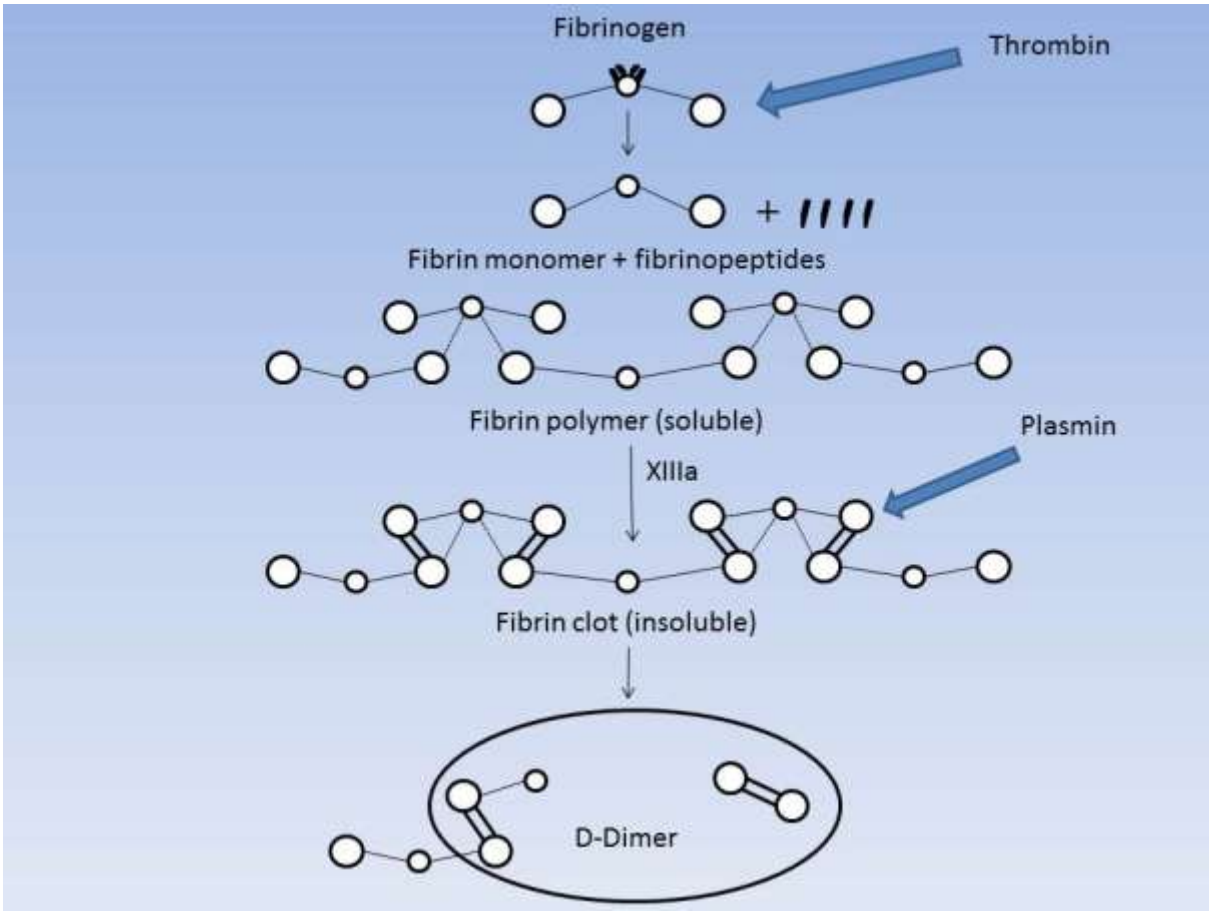

Figure 2.14 Thrombophilia D-Dimer diagram [85]

2.2.9.3 International Normalized Ratio (INR)

International normalized ratio (INR) is a calculation made to normalize prothrombin time. INR is based on the ratio of the patient's prothrombin time and the normal mean prothrombin time. Prothrombin time is a test to know how fast the blood clots in patients getting oral anticoagulant treatment [86-94]. The INR uses the ISI to equate all thromboplastins to the reference thromboplastin through the following equation:

$$INR = \left(\frac{patient\ PT}{mean\ normal\ PT}\right)^{ISI} \quad \text{.....Eq. (3)}$$

Therefore, the INR can be determined using the working prothrombin time ratio once the ISI of the thromboplastin is known.

2.2.10 X-ray Diffraction (XRD) analysis

Powder X-ray diffractometry was carried out at TUBITAK-MAM-Gebze, using a Shimadzu XRD-6000 model diffractometer with Cu X-ray tube (λ=1.5405 A° (10^{-10} meter)).

The crystallinity index is calculated by the technique based on the method proposed by Jawarska et al [95]. It consisted of measuring the maximum intensity, I_{110}, at 2θ=16°. The crystallinity index was calculated using:

$$CrlPeak = \frac{I110 - Iam}{I110} \text{.....Eq. (3)}$$

CHAPTER 3 RESULTS AND DISCUSSION

The scaffolds prepared were freeze dried in -20°C and -80°C for each concentration and for the 3% SF w/v it was mixed with methylene bisacrylamide $C_7H_{10}N_2O_2$ as a crosslinker, 3 samples with different proportions were prepared, these three proportions were prepared for both -80°C and -20°C for a total of 6 samples as shown in Table.2

Table.2 List of samples

Sample	$C_7H_{10}N_2O_2$Crosslinker volume	Freezing Temperature.	SF Volume	SF Concentration
SF20	0µl	-20°C	4.25 ml SF	3%
SF2050	50µl			
SF20300	300µl			
SF80	0µl	-80°C		
SF8050	50µl			
SF80300	300µl			

Six samples with different properties were used for each solution, six for the Acetic Buffer solution (Sf80, Sf8050, Sf80300, Sf20, Sf2050 and Sf20300) and six more for the Phosphate Buffer Saline solution (Sf80, Sf8050, Sf80300, Sf20, Sf2050 and Sf20300).

The results of the swelling test for all of the samples within the same solution (ABS or PBS) showed that after a period of time they reached the equilibrium swelling ratio no matter what solution was used; however the response of the samples in the same solution was different depending on the crosslinking and the preparation temperature -80°C or -20°C as shown in Table.3 and Table.6

For the swelling test the scaffolds were soaked in ABS and PBS solutions and the swelling ratio was observed until it reached a stable value as shown in the tables below.

3.1 Swelling test

3.1.1 Phosphate Buffer Saline (PBS) Solution pH (7.4)

Table.3 Silk Fibroin Scaffolds weight while swelling in Phosphate Buffer Saline Solution pH (7.4)

Time(Hours)	-20°C			-80°C		
	SF20 weight(g)	SF2050 weight(g)	SF20300 weight(g)	SF80 weight(g)	SF8050 weight(g)	SF80300 weight(g)
0	0.0669	0.0606	0.0497	0.0563	0.0569	0.0511
0.25	0.6880	0.4666	0.3409	0.6745	0.6845	0.6512
0.5	0.7374	0.4875	0.3679	0.6886	0.7128	0.6628
0.75	0.7461	0.5094	0.3720	0.7352	0.7372	0.6674
1	0.7818	0.5176	0.3871	0.7520	0.7552	0.6795
1.5	0.8139	0.5226	0.4088	0.7592	0.7583	0.7091
2	0.8221	0.5486	0.4307	0.7883	0.7943	0.7063
2.5	0.8298	0.5527	0.4112	0.7977	0.7993	0.7201
3.5	0.8311	0.5525	0.4130	0.7993	0.7725	0.7077
24	0.8756	0.5873	0.4296	0.8518	0.8006	0.7594
27	0.9083	0.6161	0.4322	0.8692	0.8225	0.7580
48	0.9095	0.6168	0.4376	0.8793	0.8374	0.7726
96	1.0055	0.7103	0.5017	0.9152	0.8886	0.8392
120	1.0058	0.7123	0.5021	0.9155	0.8887	0.8396

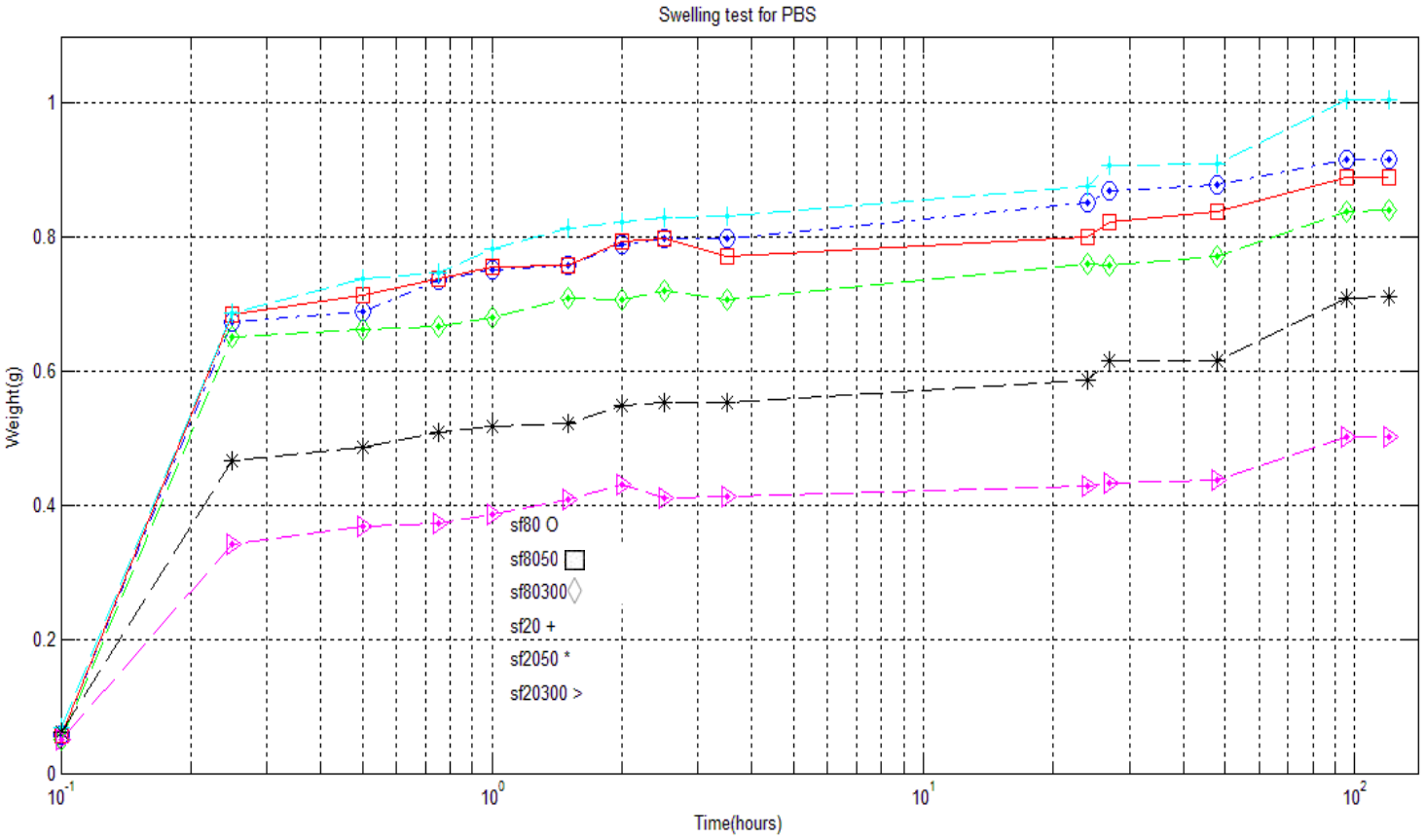

Figure 3.1 Plot of the swelling values for PBS

Table.4 Standard Deviation of Silk Fibroin Scaffolds in PBS Solution pH (7.4)

Scaffold no.	Number of values:	Mean (Average):	Standard deviation:	Variance(Standard deviation):	Population Standard deviation:	Variance(Population Standard deviation):
Sf20	14	0.78727	0.22726	0.05165	0.21899	0.04796
Sf2050	14	0.53292	0.15492	0.024	0.14929	0.02229
Sf20300	14	0.39175	0.10836	0.01174	0.10442	0.0109
Sf80	14	0.74872	0.2136	0.04562	0.20583	0.04237
Sf8050	14	0.73634	0.20428	0.04173	0.19685	0.03875
Sf80300	14	0.68029	0.19065	0.03635	0.18371	0.03375

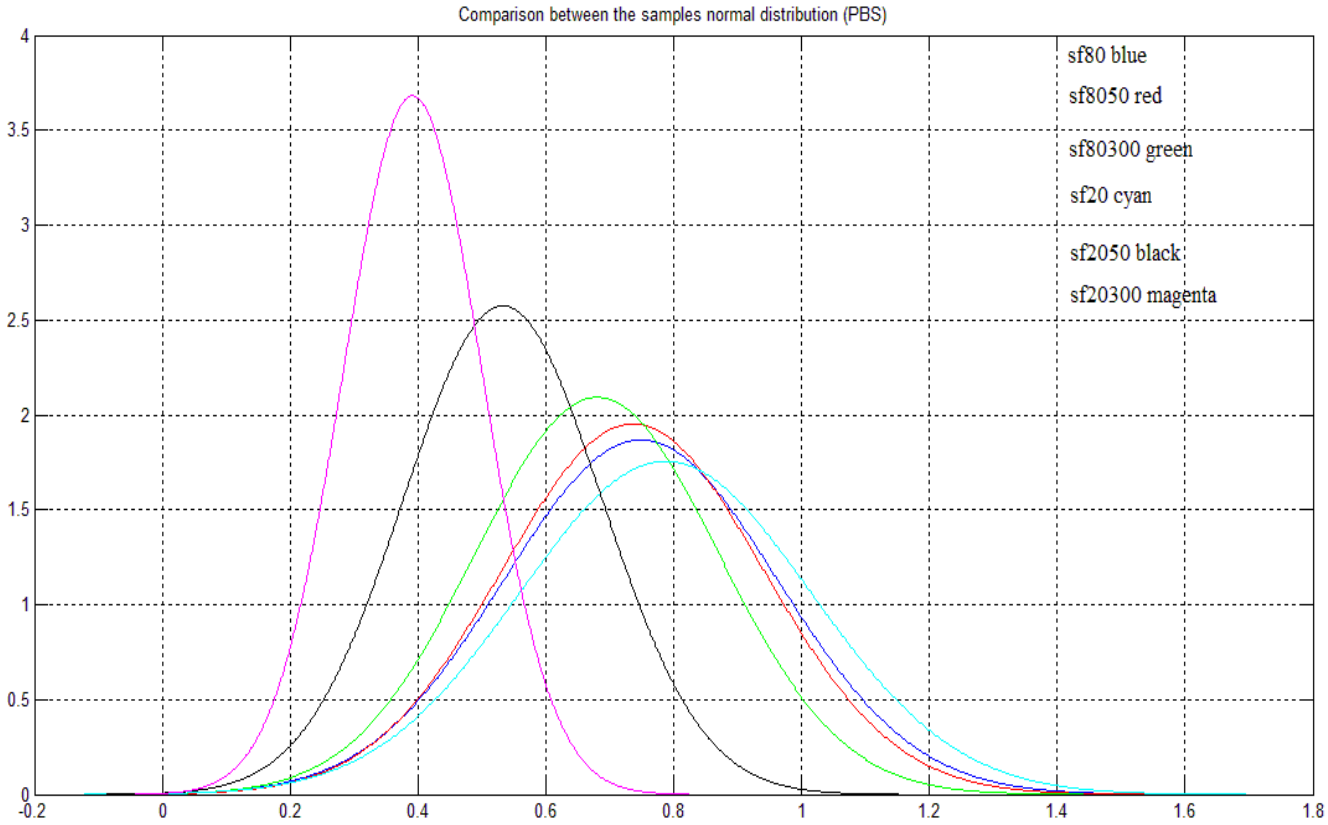

Figure 3.2 Normal distribution of the samples

The swelling ratios can be calculated by applying Eq. (1)

By applying this equation to the measured values a table of swelling ratios is obtained:

Table.5 Silk Fibroin Scaffolds swelling ratios in PBS Solution pH (7.4)

Time(Hours)	-20°C			-80°C		
	SF20 weight increase Percentage	SF2050 weight increase Percentage	SF20300 weight increase Percentage	SF80 weight increase Percentage	SF8050 weight increase Percentage	SF80300 weight increase Percentage
0	0	0	0	0	0	0
0.25	928.4	670	585.9	1098	1103	1174.4
0.5	1002.2	704.5	640.2	1123.1	1152.7	1197.1
0.75	1015.2	740.6	648.5	1205.9	1195.6	1206.1
1	1068.6	754.1	678.8	1235.7	1227.2	1229.7
1.5	1116.6	762.4	722.5	1248.5	1232.7	1287.7
2	1128.8	805.3	766.6	1300.2	1296	1282.2
2.5	1140.4	812	727.3	1316.9	1304.7	1309.2
3.5	1142.3	811.7	730.9	1319.7	1257.6	1284.9
24	1208.8	869.1	764.3	1413	1307	1386.1
27	1257.7	916.7	769.6	1443.9	1345.5	1383.4
48	1259.5	917.8	780.4	1461.8	1371.7	1411.9
96	1403	1072.1	909.4	1525.6	1461.7	1542.3
120	1403.4	1075.4	910.2	1526.1	1461.9	1543.1

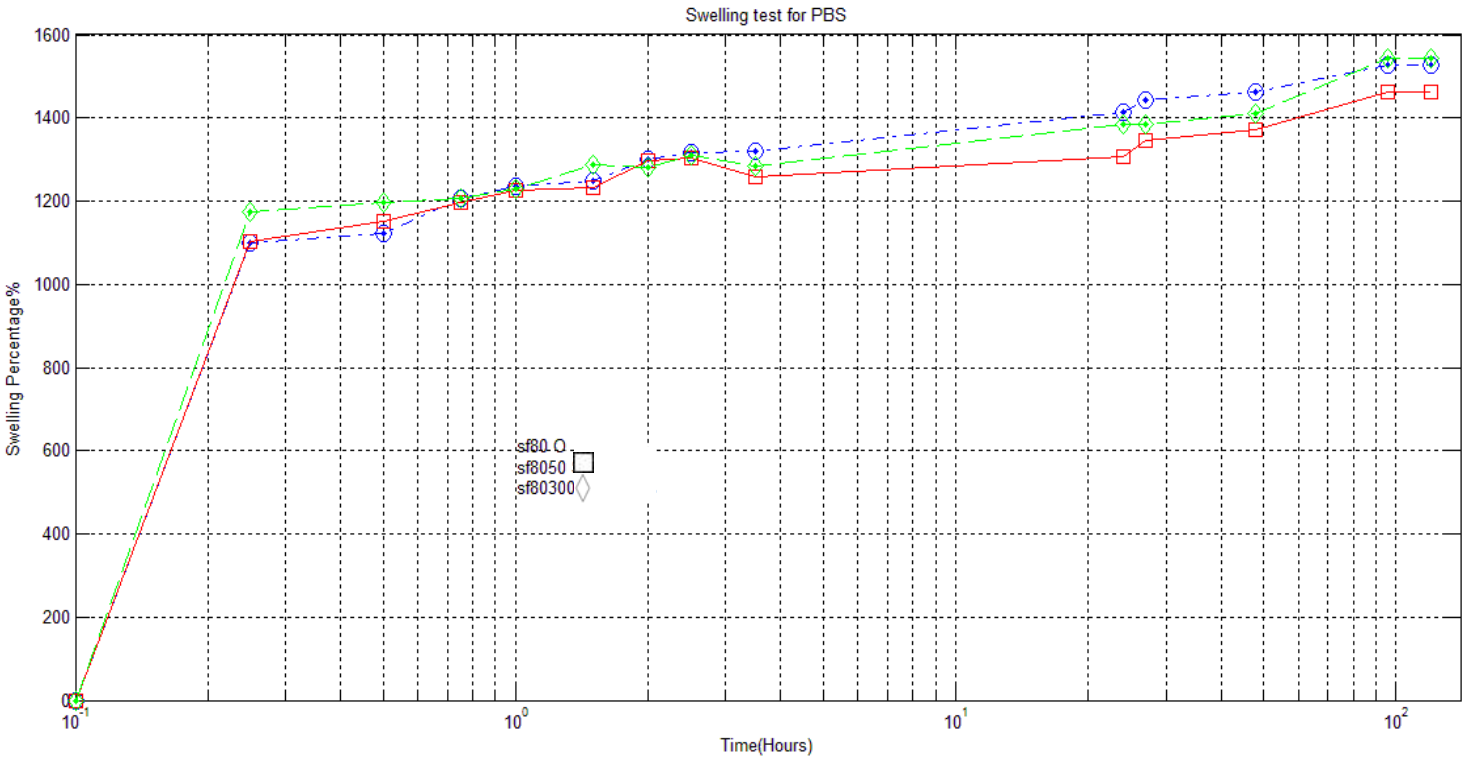

Figure 3.3 Silk fibroin scaffolds prepared at -80°C swelling ratios in PBS solution pH (7.4)

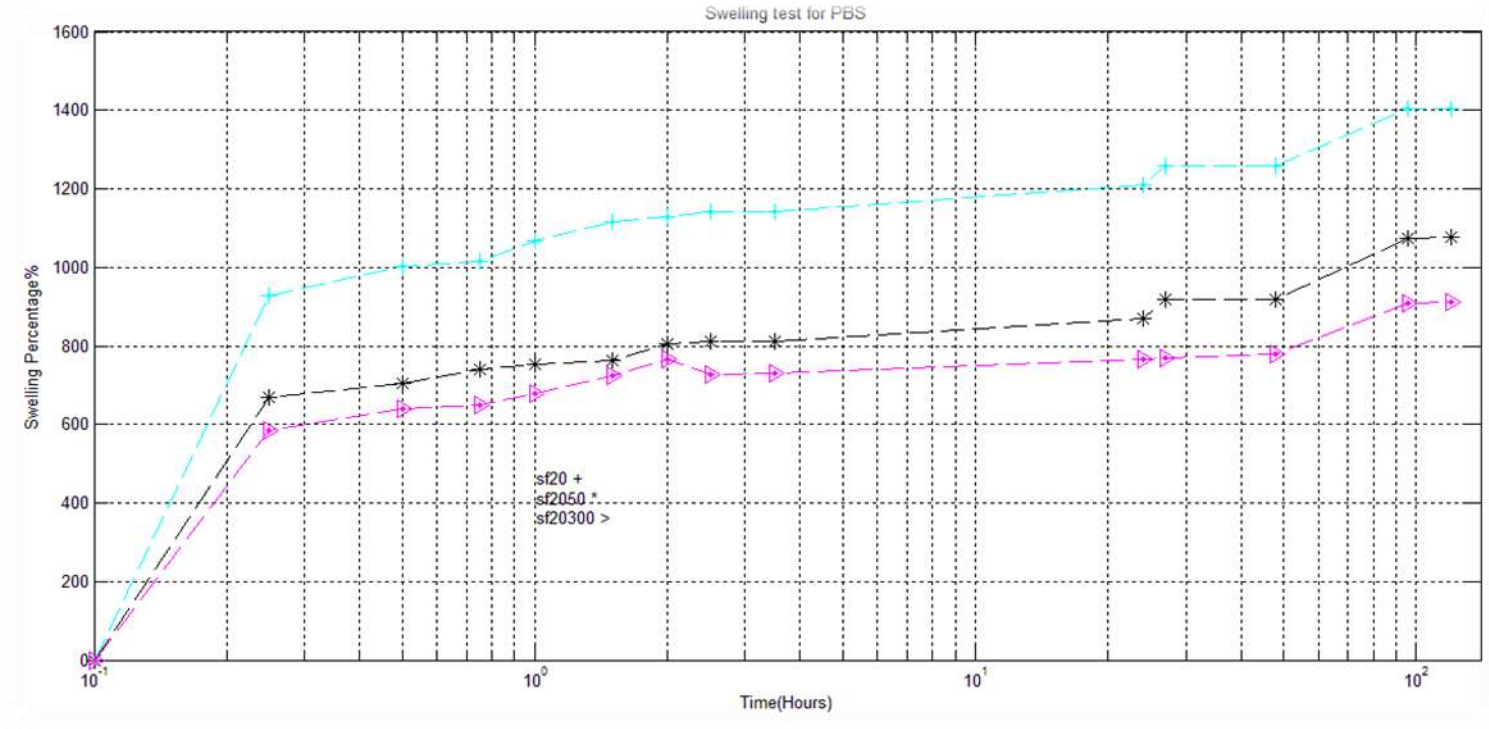

Figure 3.4 Silk fibroin scaffolds prepared at -20°C swelling ratios in PBS solution pH (7.4)

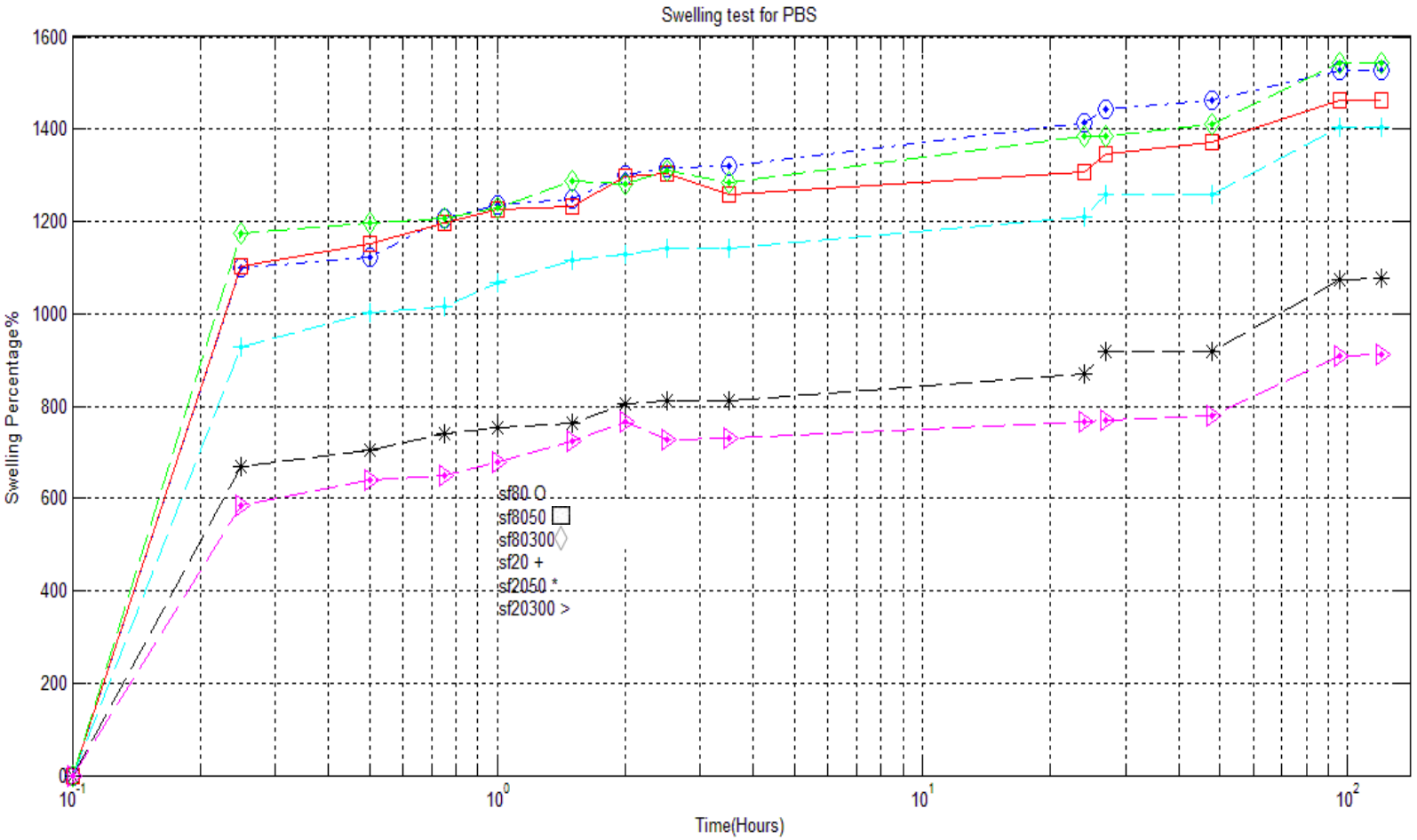

Figure 3.5 Silk fibroin scaffolds prepared swelling ratios in PBS solution pH (7.4)

For the PBS solution sample (Sf20300) which is SF with the highest crosslinking amount it gave an increase in terms of swelling until it reached its final value, however it had the lowest swelling ratio compared to the low crosslinked SF scaffold and the pure SF scaffold (Sf2050 & Sf20) which were prepared at -20°C which indicates that as we increase the crosslinker in the scaffold the swelling ratio decreases as shown in Figure 3.4

As for the scaffolds prepared at -80°C the crosslinking didn't have that much of an effect on the swelling ratios. For the comparison between the scaffolds prepared at -80°C and the scaffolds prepared at -20°C, the scaffolds prepared at -80°C had a rapid swelling and their final swelling ratios surpasses all the other scaffolds prepared at -20°C this is related to the pore sizes which are inversely related to the freezing temperature as it decreases the pore size increases. The responses are shown in Figure 3.5

3.1.2 Acetic Buffer Solution (ABS) Solution pH (1.2)

Table.6 Silk Fibroin Scaffolds weights while swelling in Acetic Buffer Solution pH (1.2)

Time(Hours)	-20°C			-80°C		
	SF20 weight(g)	SF2050 weight(g)	SF20300 weight(g)	SF20 weight(g)	SF2050 weight(g)	SF20300 weight(g)
0	0.0621	0.0704	0.0688	0.0732	0.0642	0.0805
0.25	0.6206	0.6831	0.5967	0.9323	0.8025	0.8369
0.5	0.6498	0.7296	0.6436	0.9785	0.8462	0.8683
0.75	0.6763	0.7495	0.6532	0.9987	0.8625	0.8903
1	0.7056	0.7779	0.6653	1.0093	0.8653	0.9165
1.5	0.7140	0.7950	0.6753	1.0317	0.8663	0.9241
2	0.7173	0.7947	0.6746	1.0321	0.8672	0.9245
2.5	0.7177	0.7969	0.6792	1.0327	0.8684	0.9262
3	0.7178	0.7973	0.6791	1.0334	0.8693	0.9269
24	0.7662	0.8243	0.7309	1.0956	0.9170	0.9803
72	0.7628	0.8443	0.7432	1.1432	0.9350	0.9972
96	0.7772	0.8690	0.7685	1.1565	0.9362	1.0071
120	0.7663	0.8532	0.7588	1.1503	0.936	0.9902
144	0.7853	0.8693	0.7637	1.1514	0.9375	0.9948
168	0.7848	0.8649	0.7645	1.1522	0.9382	0.9987

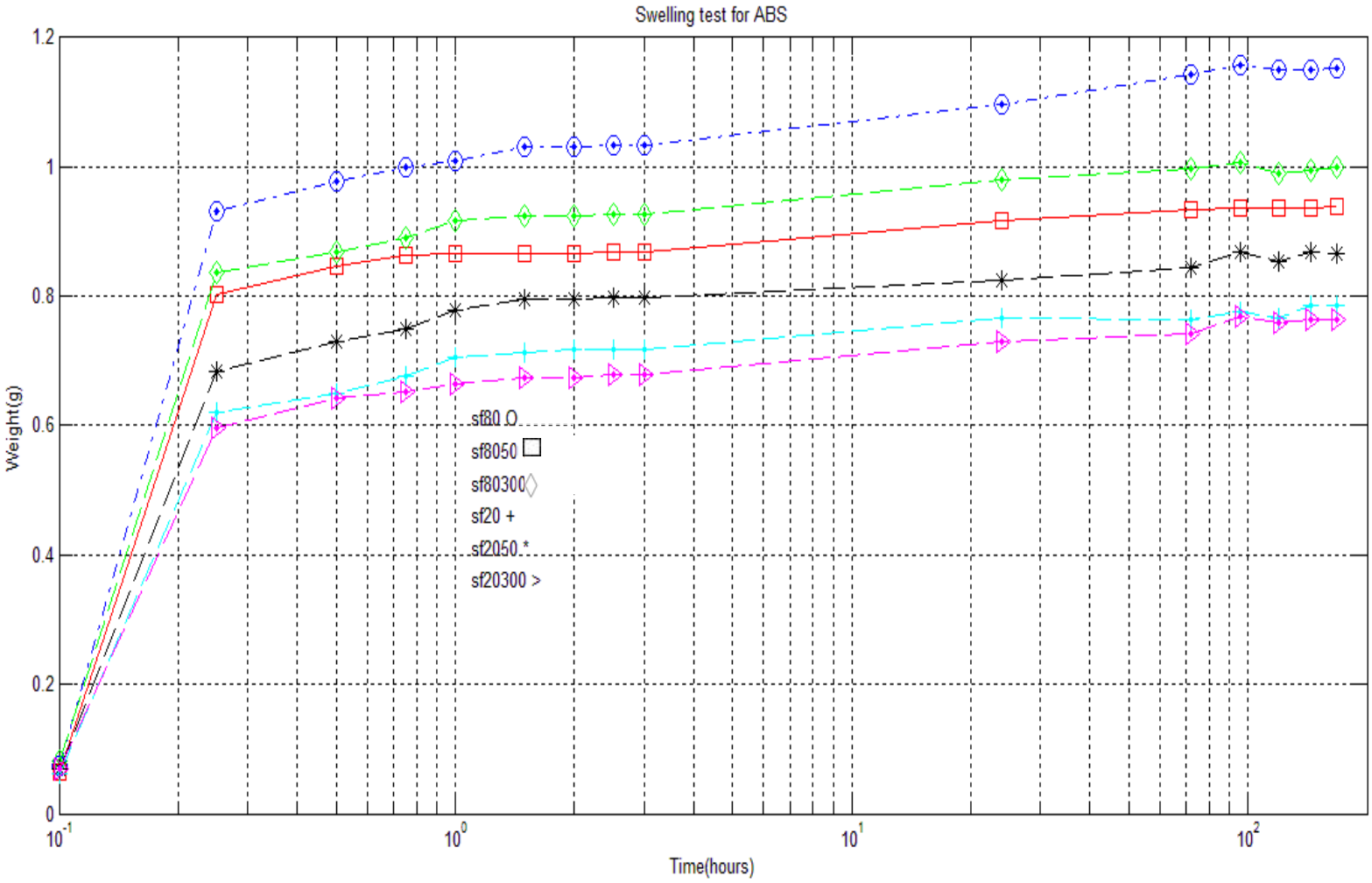

Figure 3.6 Plot of the swelling values for ABS

Table.7 Standard Deviation of Silk Fibroin Scaffolds in ABS Solution pH (1.2)

Scaffold no.	Number of values:	Mean (Average):	Standard deviation:	Variance(Standard deviation):	Population Standard deviation:	Variance(Population Standard deviation):
Sf20	15	0.68159	0.17839	0.03182	0.17234	0.0297
Sf2050	15	0.75463	0.19682	0.03874	0.19014	0.03615
Sf20300	15	0.65769	0.17116	0.02929	0.16535	0.02734
Sf80	15	0.99807	0.26607	0.07079	0.25704	0.06607
Sf8050	15	0.83412	0.21706	0.04711	0.2097	0.04397
Sf80300	15	0.88417	0.22835	0.05214	0.2206	0.04867

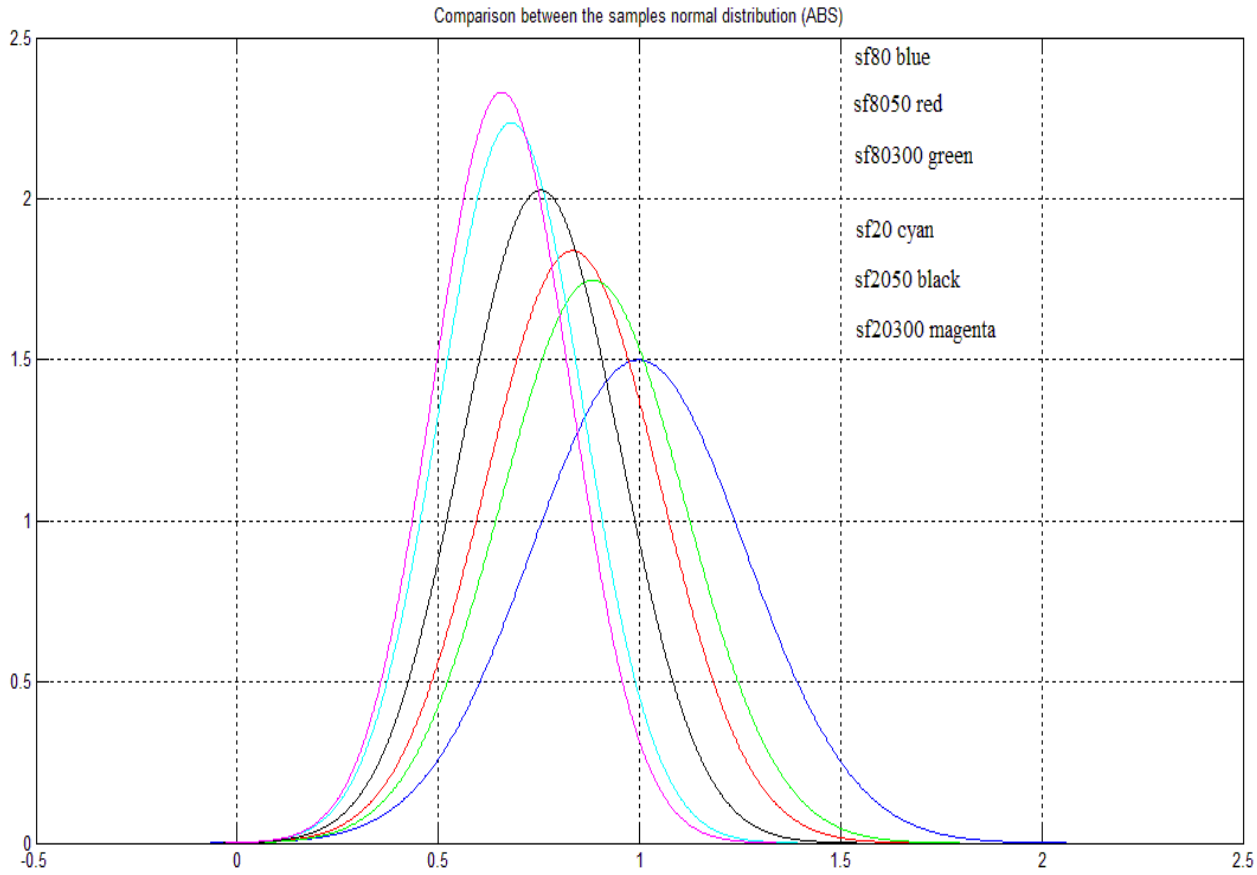

Figure 3.7 Normal distribution of the samples

The swelling ratios can be calculated by applying Eq(1)

By applying this equation to the measured values a table of swelling ratios is obtained:

Table.8 Silk Fibroin Scaffolds swelling ratios in ABS Solution pH (1.2)

Time(Hours)	-20°C			-80°C		
	Sf20 weight increase percentage	Sf2050 weight increase percentage	Sf20300 weight increase percentage	Sf80 weight increase percentage	Sf8050 weight increase percentage	Sf80300 weight increase percentage
0	0	0	0	0	0	0
0.25	899.4	870.3	767.3	1173.6	1150	939.6
0.5	946.4	936.4	835.5	1236.7	1218.1	978.6
0.75	989	964.6	849.4	1264.3	1243.5	1006
1	1036.2	1005	867	1278.8	1247.8	1038.5
1.5	1049.8	1029.3	881.5	1309.4	1249.4	1048
2	1055.1	1028.8	880.5	1310	1250.8	1048.4
2.5	1055.7	1032	887.2	1310.8	1252.6	1050.6
3	1055.9	1032.5	887.1	1311.7	1254	1051.4
24	1133.8	1070.9	962.4	1396.7	1328.3	1117.8
72	1128.3	1099.3	980.2	1461.7	1356.4	1138.8
96	1151.5	1134.4	1017	1479.9	1358.3	1151.1
120	1134	1111.9	1002.9	1471.4	1357.9	1130.1
144	1164.6	1134.8	1010	1473	1360.3	1135.8
168	1163.8	1128.6	1011.2	1474	1361.4	1140.6

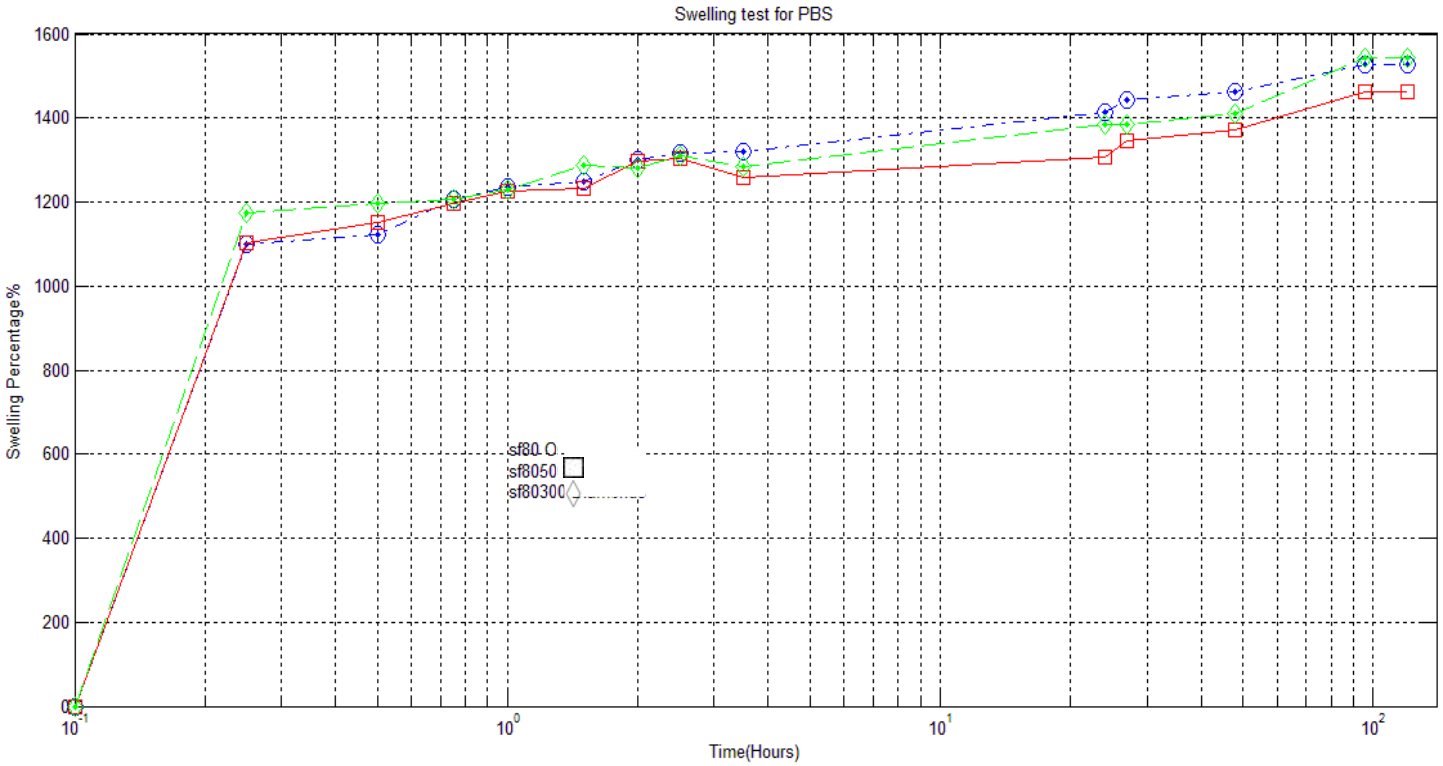

Figure 3.8 Silk fibroin scaffolds prepared at -80°C swelling ratios in ABS solution pH (1.2)

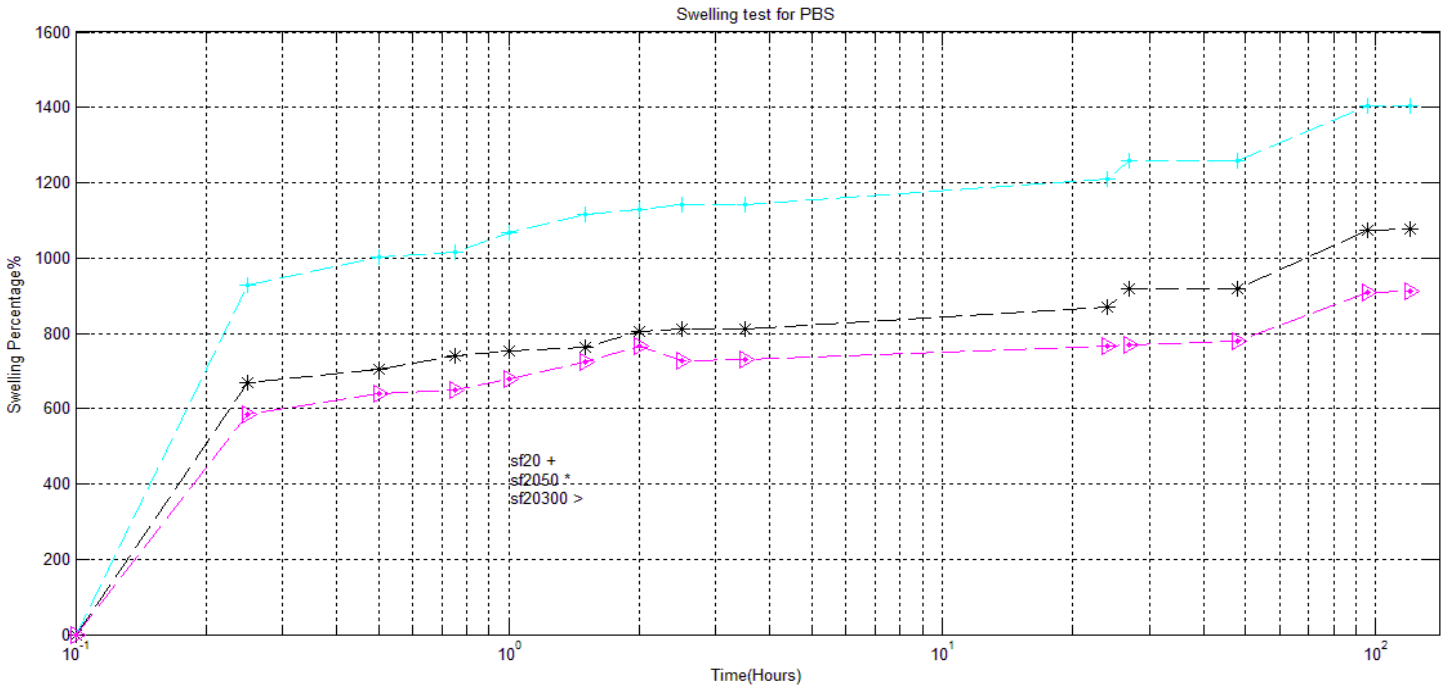

Figure 3.9 Silk fibroin scaffolds prepared at -20°C swelling ratios in ABS solution pH (1.2)

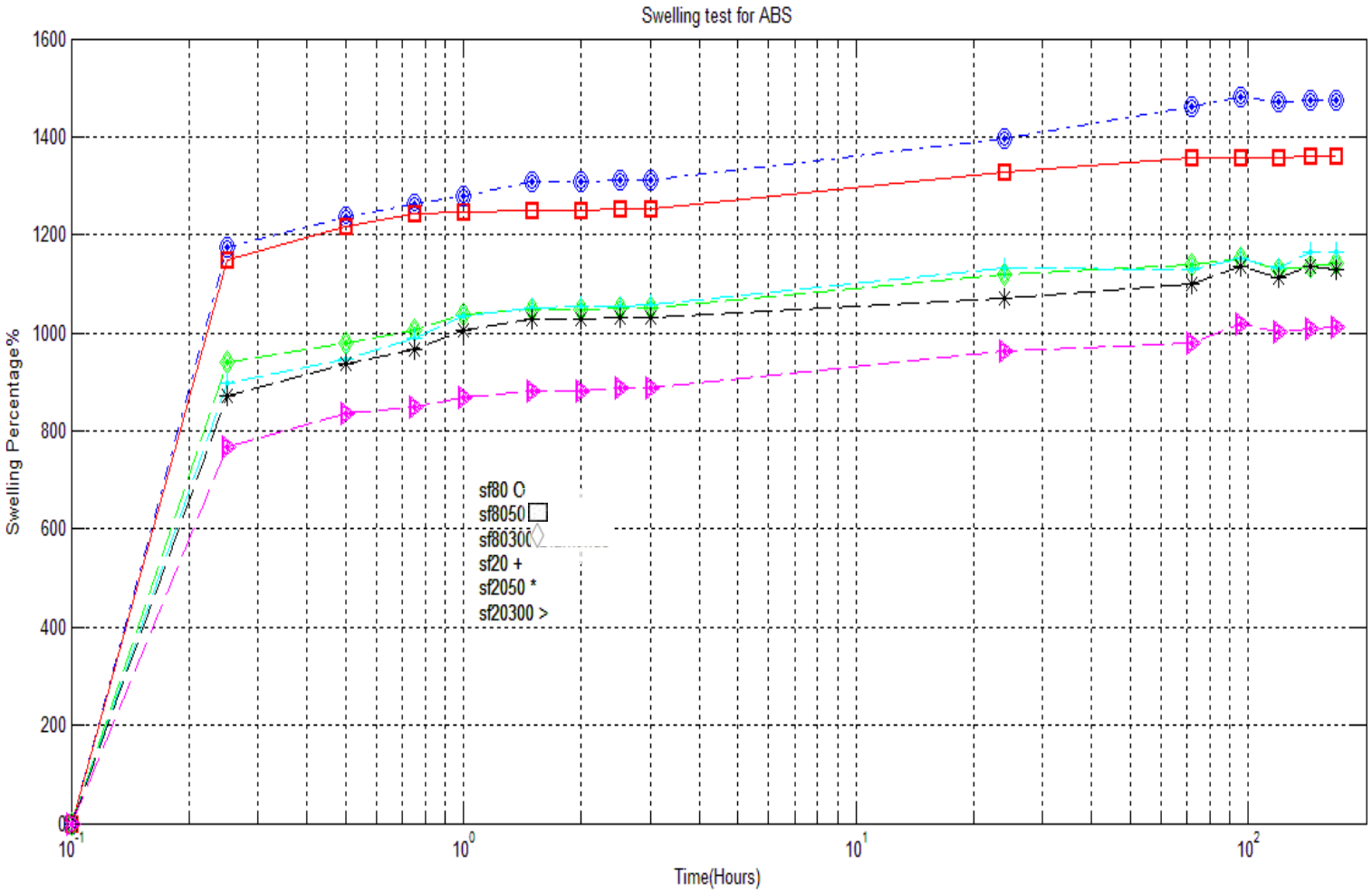

Figure 3.10 Silk fibroin scaffolds prepared swelling ratios in ABS solution pH (1.2)

For the ABS solution sample (Sf20) which is pure SF without a crosslinker it gave an increase in terms of swelling until it reached its final value, however it had the highest swelling ratio compared to the low crosslinked SF scaffold and the highly crosslinked SF scaffold (Sf2050 & Sf20300) which were prepared at -20°C as well, which indicates that as we increase the crosslinker in the scaffold the equilibrium swelling ratio decreases as shown in figure 3.9

As for the scaffolds prepared at -80°C the crosslinking had an effect on the swelling ratios which is inversely related as the crosslinker increases in the scaffold the swelling ratio decreases. But by comparison the scaffolds prepared at -80°C had a rapid swelling and their final swelling ratios surpasses all the other scaffolds prepared at -20°C as shown in figure 3.9this is also related to the pore sizes as in the ABS test which are inversely related to the freezing temperature as it decreases the pore size increases. The responses are shown in Figure 3.10, however for all the

samples in the PBS solution they approached their equilibrium swelling ratio R_{se} within72 hours as shown in Table.5 and it took 96 hours for the samples in the ABS solution to approach their R_{se} as shown in Table.8

3.2 Biodegradation test with protease enzyme

For the biodegradation test a solution of protease and water was used with 0.3 g/ml concentration and the scaffolds were tested against the protease solution at 37°C to match with the body's temperature.

Table.9 Silk Fibroin Scaffolds Weight while degrading in the Protease Solution

Time	-20°C			-80°C		
	Sf20 weight(g)	Sf2050 weight(g)	Sf20300 weight(g)	Sf80 weight(g)	Sf8050 weight(g)	Sf80300 weight(g)
0	0.9450	0.9520	0.9830	1.1790	1.1360	0.9730
0.25	0.9292	0.9371	0.9686	1.1628	1.1216	0.9616
0.5	0.9142	0.9230	0.9552	1.1461	1.1088	0.9529
0.75	0.8971	0.9077	0.9403	1.1285	1.0953	0.9453
1	0.8809	0.8934	0.9254	1.1100	1.0818	0.9361
1.5	0.8479	0.8656	0.8978	1.0768	1.0626	0.9177
2	0.8176	0.8350	0.8696	1.0454	1.0352	0.8993
2.5	0.7875	0.8076	0.8408	1.0135	1.0084	0.8757
3	0.7570	0.7765	0.8121	0.9800	0.9807	0.8603
17	0.0161	0.0751	0.1344	0.2158	0.2423	0.2423
18	0	0.0154	0.0747	0.1486	0.1829	0.1995
19	0	0	0.0143	0.0817	0.1284	0.1480
20	0	0	0	0.0170	0.0704	0.1002
21	0	0	0	0	0.0150	0.0499
22	0	0	0	0	0	0.0117
23	0	0	0	0	0	0

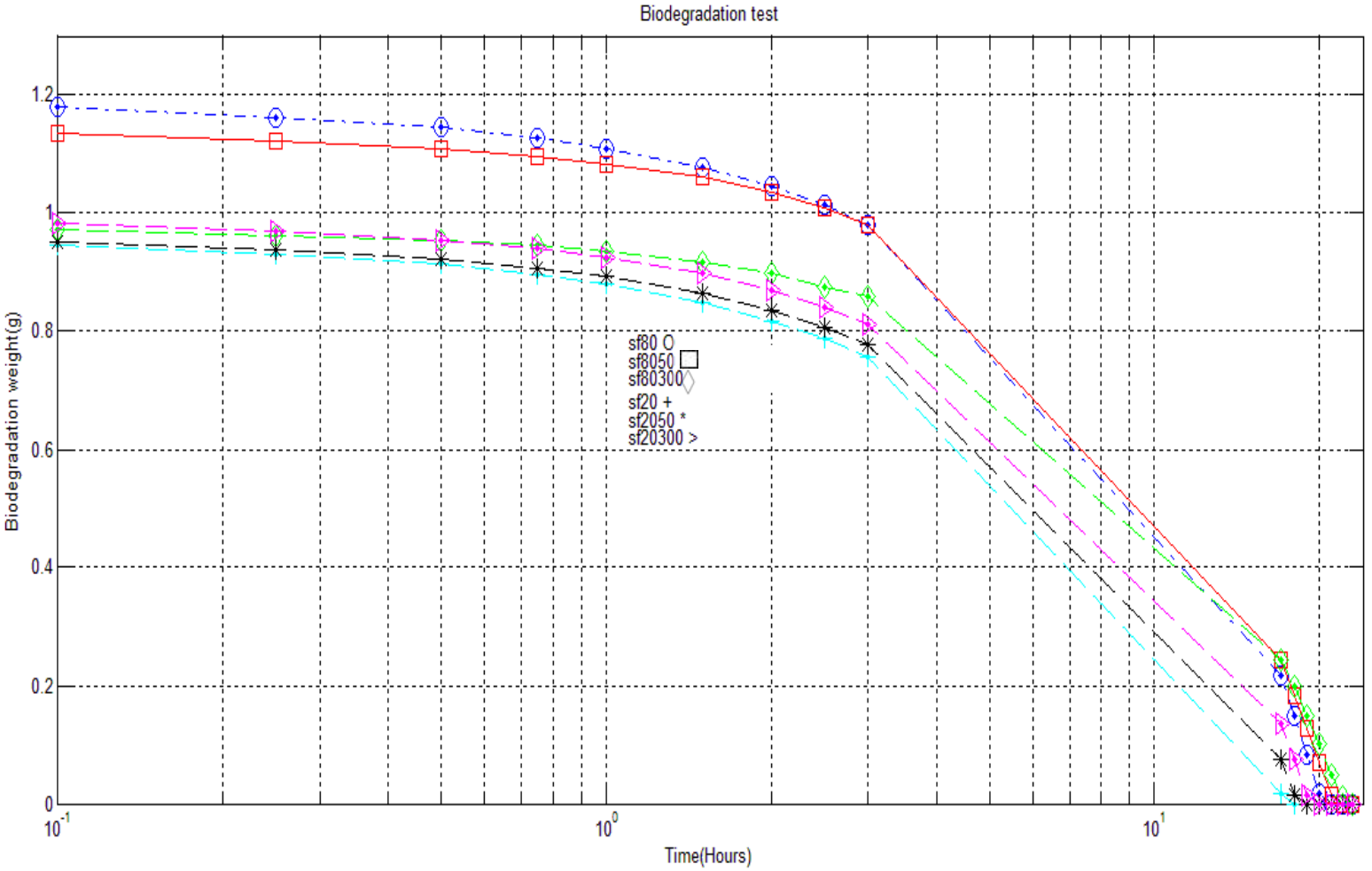

Figure 3.11 Plot of the values for the biodegradation

Table 10 Standard Deviation of Silk Fibroin Scaffolds in Protease Solution

Scaffold no.	Number of values:	Mean (Average):	Standard deviation:	Variance(Standard deviation):	Population Standard deviation:	Variance(Population Standard deviation):
Sf20	16	0.48703	0.44412	0.19724	0.43002	0.18492
Sf2050	16	0.49928	0.44554	0.19851	0.43139	0.1861
Sf20300	16	0.52601	0.45335	0.20553	0.43896	0.19268
Sf80	16	0.64407	0.53164	0.28264	0.51475	0.26497
Sf8050	16	0.64184	0.50661	0.25666	0.49053	0.24061
Sf80300	16	0.56709	0.42385	0.17965	0.41039	0.16842

Comparison between the samples normal distribution (Biodegradation)

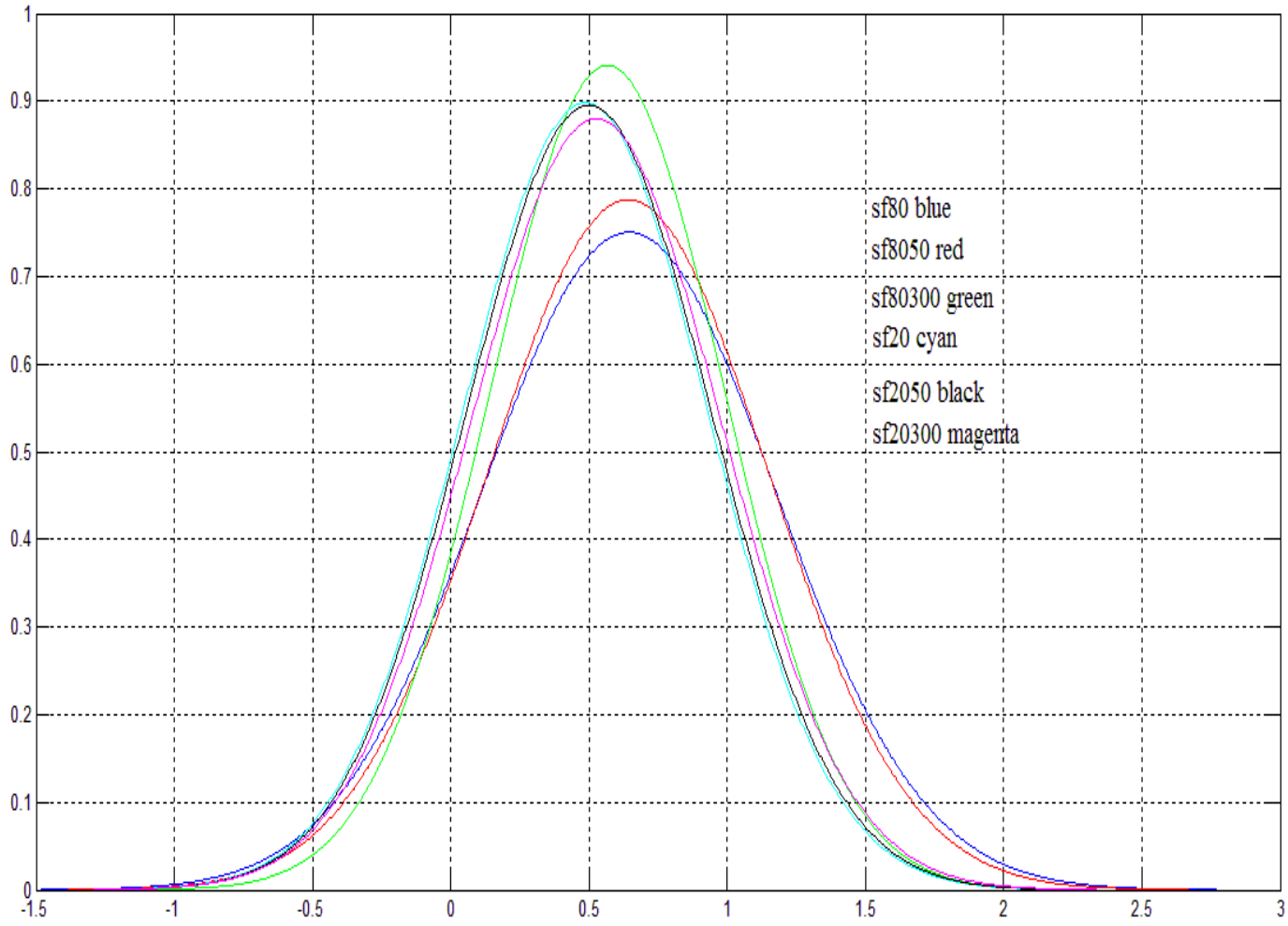

Figure 3.12 Normal distribution of the samples

The biodegradation percentage can be calculated by applying Eq.(2)

Table.11 Biodegradation Percentage of Silk Fibroin Scaffolds in Protease Solution

Time(Hour)	Sf20	Sf2050	Sf20300	Sf80	Sf8050	Sf80300
0	100	100	100	100	100	100
0.25	98.3280	98.4349	98.5351	98.6260	98.7324	98.8284
0.5	96.7407	96.9538	97.1719	97.2095	97.6056	97.9342
0.75	94.9312	95.3466	95.6562	95.7167	96.4173	97.1531
1	93.2169	93.8445	94.1404	94.1476	95.2289	96.2076
1.5	89.7249	90.9244	91.3327	91.3316	93.5387	94.3165
2	86.5185	87.7101	88.4639	88.6684	91.1268	92.4255
2.5	83.3333	84.8319	85.5341	85.9627	88.7676	90.0000
3	80.1058	81.5651	82.6144	83.1213	86.3292	88.4173
17	1.7037	7.8887	13.6724	18.3036	21.3292	24.9024
18	0	1.6176	7.5992	12.6039	16.1004	20.5036
19	0	0	1.4547	6.9296	11.3028	15.2107
20	0	0	0	1.4419	6.1972	10.2980
21	0	0	0	0	1.3204	5.1285
22	0	0	0	0	0	1.2025
23	0	0	0	0	0	0

It is shown that in Table.10 how much each scaffold has lost from its original weight obviously the crosslinking delays the biodegradation of the scaffold as the highly crosslinked scaffold lasted longer than the others. Another factor is the preparation temperature the scaffolds prepared at -20°C namely (Sf20, Sf2050, and Sf20300) degraded faster than the others prepared at -80°C (Sf80, Sf8050 and Sf80300), however within any three of these samples the crosslinker played a crucial role in delaying the biodegradation as shown in figure 3.15

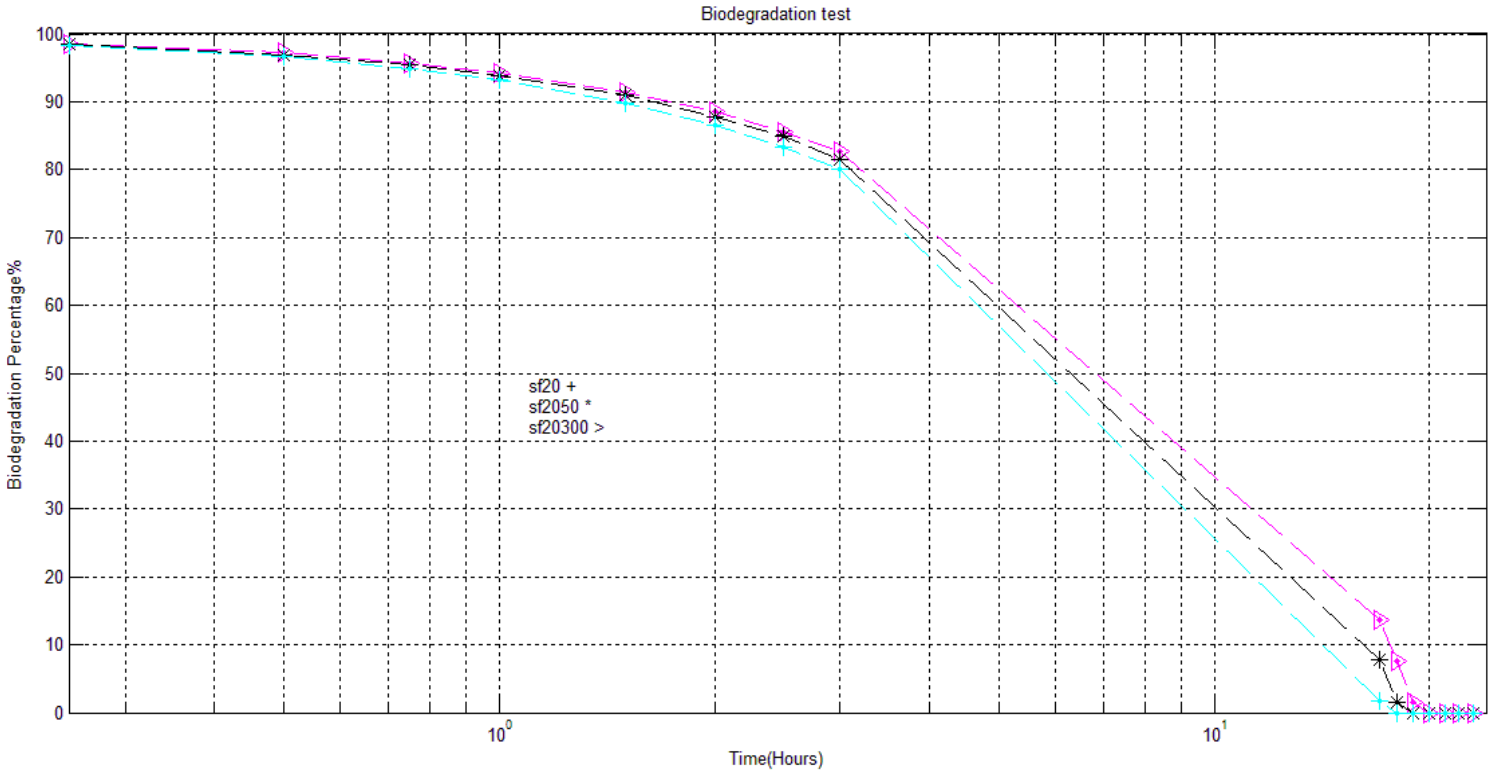

Figure 3.13 Biodegradation percentage of silk fibroin scaffold prepared at -20°C

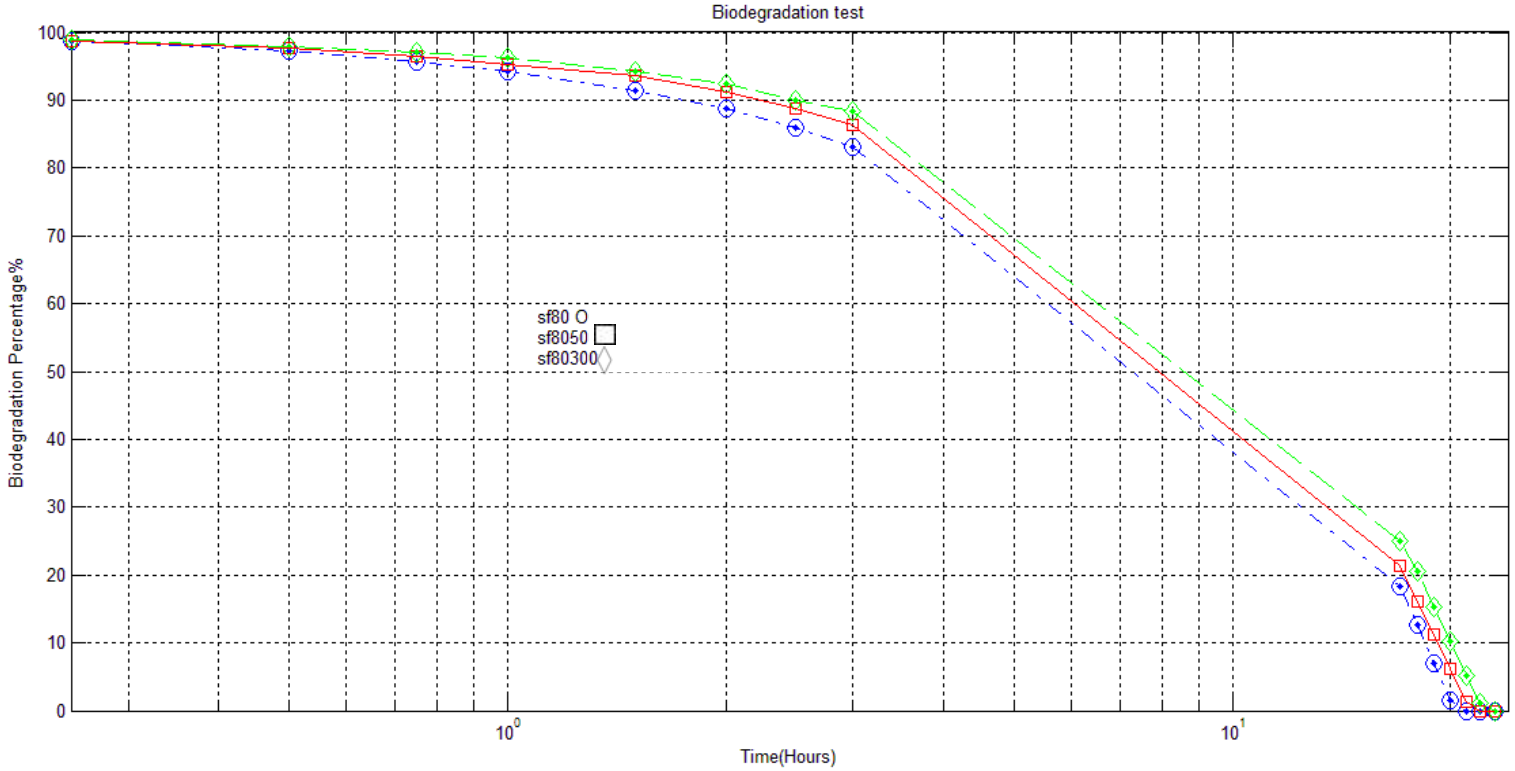

Figure 3.14 Biodegradation percentage of silk fibroin scaffold prepared at -80°C

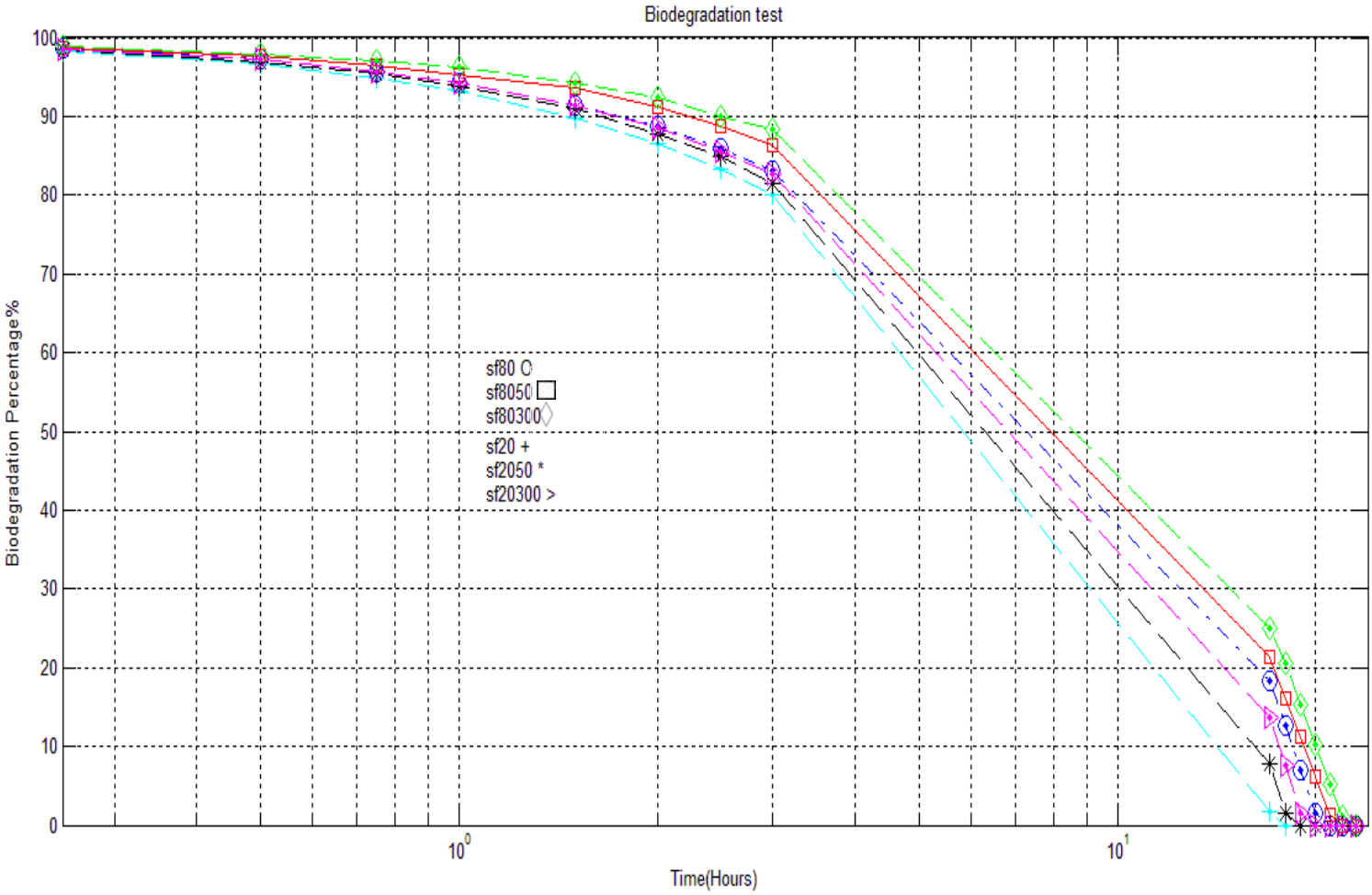

Figure 3.15 Biodegradation percentages of the scaffolds

3.3 SEM Analysis

Morphological features of raw silk fibers, degummed silk fibers, silk fibroin films and scaffolds were studied by SEM.

3.3.1 Raw silk fibers

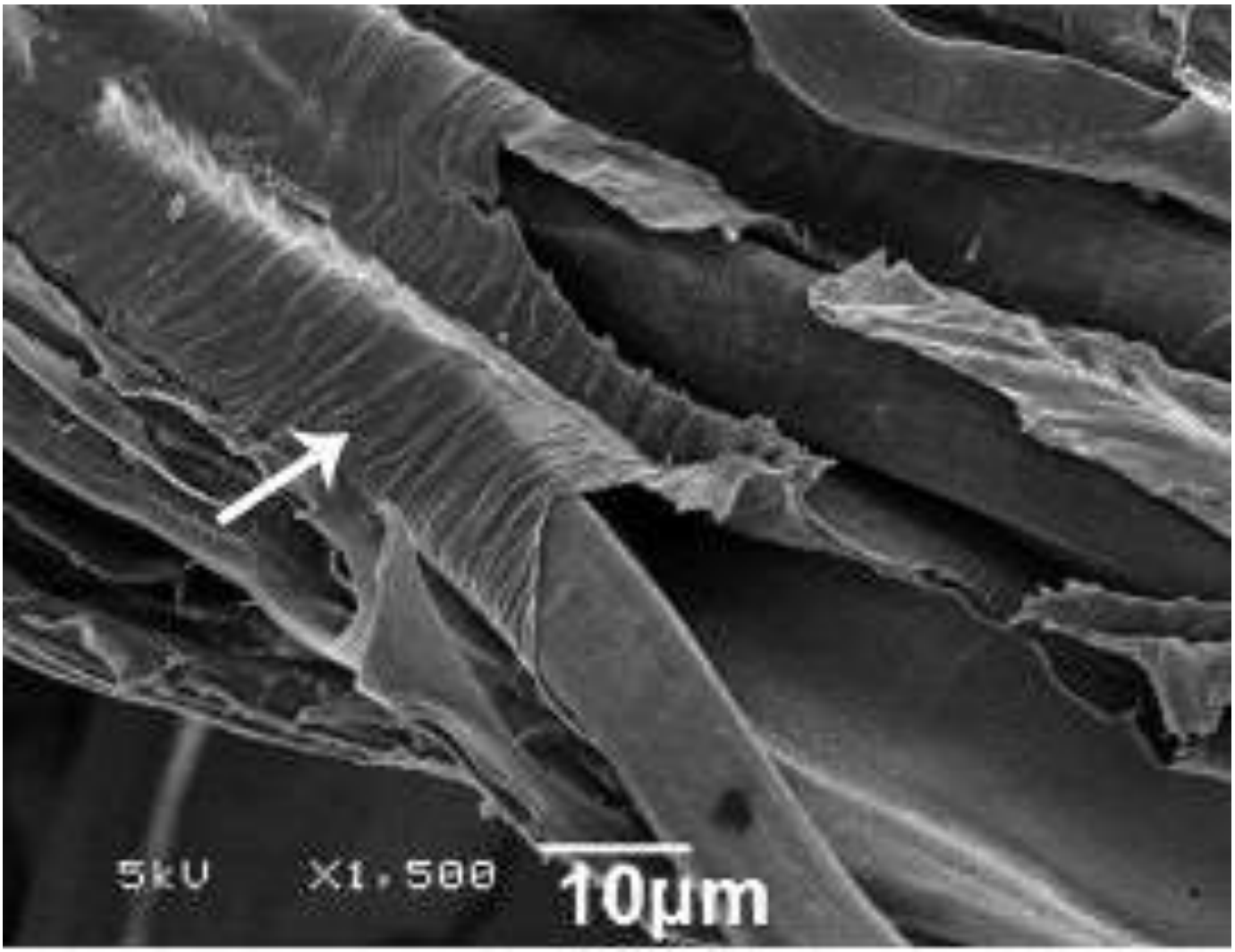

Figure 3.16 SEM Micrograph of raw silk fibers [96]

This SEM Micrograph shows the raw silk fibers coated with sericin the white arrow in Figure3.16 points to the sericin covering the fibers.

3.3.2 Degummed silk fibers

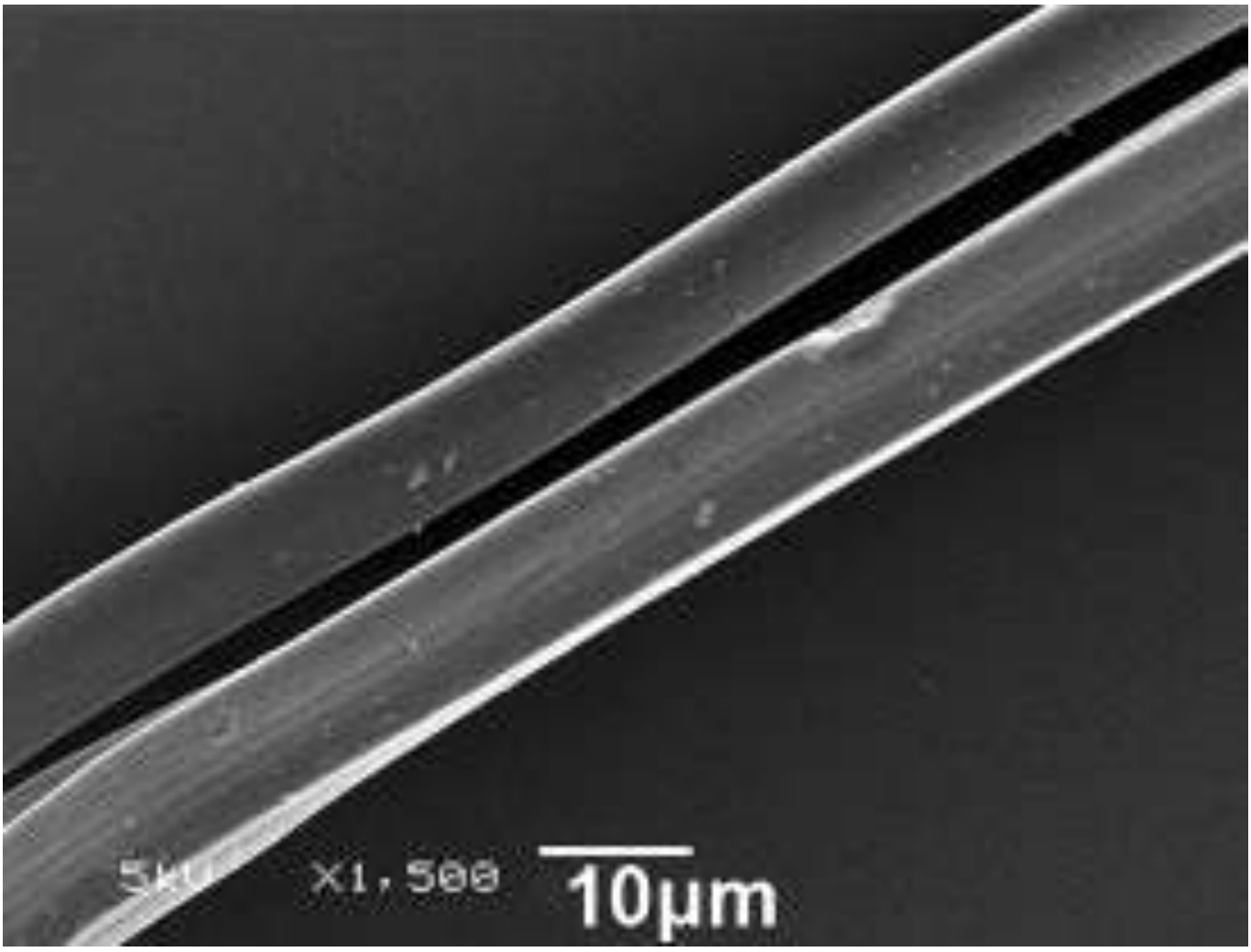

Figure 3.17 SEM Micrograph of degummed silk fibers [95]

This SEM micrograph in Figure 3.17 shows the smooth surface of the silk fibers after the degumming process and confirms the removal of the sericin protein therefore the effectiveness of the degumming process.

3.3.4 Pure Silk fibroin film

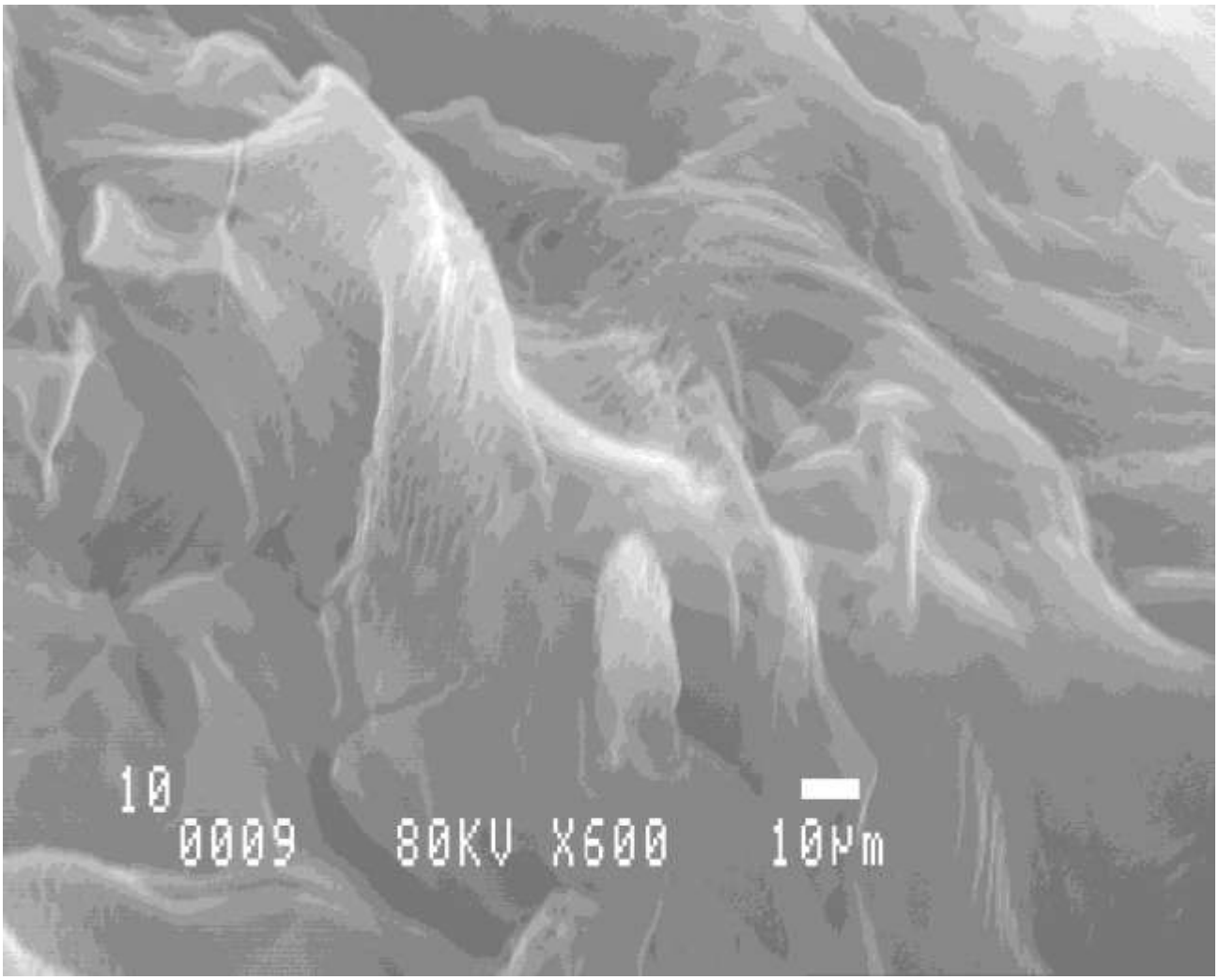

Figure 3.18 SEM Micrograph of pure silk fibroin film

This SEM micrograph in Figure 3.18 shows that the pure silk fibroin film is non-porous and has a rough surface with ridges on its surface which makes it suitable for cell culturing because cells like to cling on these surfaces.

3.3.3 Silk fibroin film crosslinked with methylene bisacrylamide $C_7H_{10}N_2O_2$

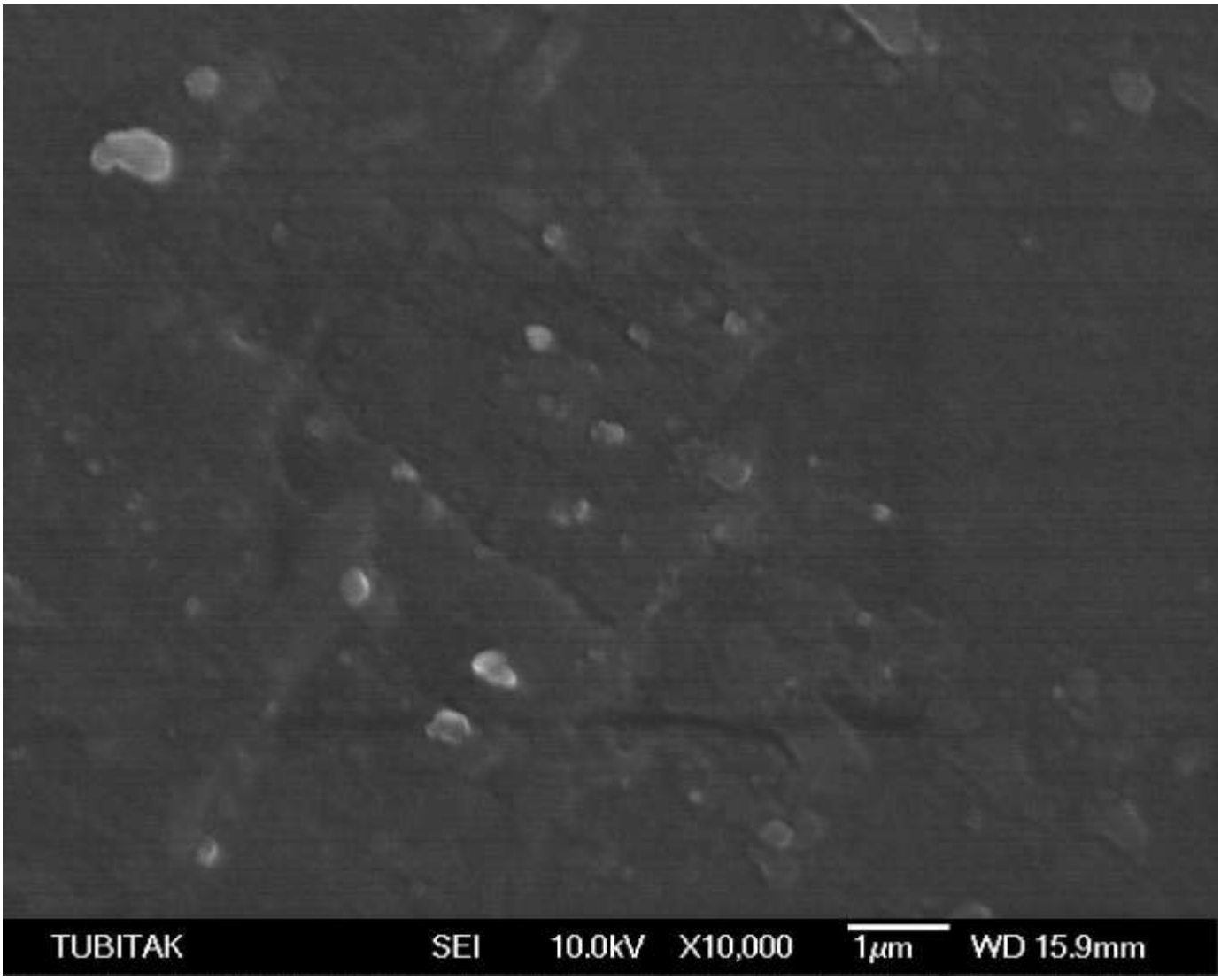

Figure 3.19 SEM Micrograph of silk fibroin film crosslinked with methylene bisacrylamide $C_7H_{10}N_2O_2$

The micrograph of the silk fibroin film shown in Figure 3.19 shows that the film is non-porous with a smooth surface with some insoluble silk fibroin particles on its surface which is an evidence of the crosslinking reactions and micro and nanoparticles formed are agglomerated crosslinked structures. This surface smoothness is owed to the crosslinker which tightens the material and brings it together resulting in a smooth surface.

3.3.5 Silk fibroin scaffold at -80°C

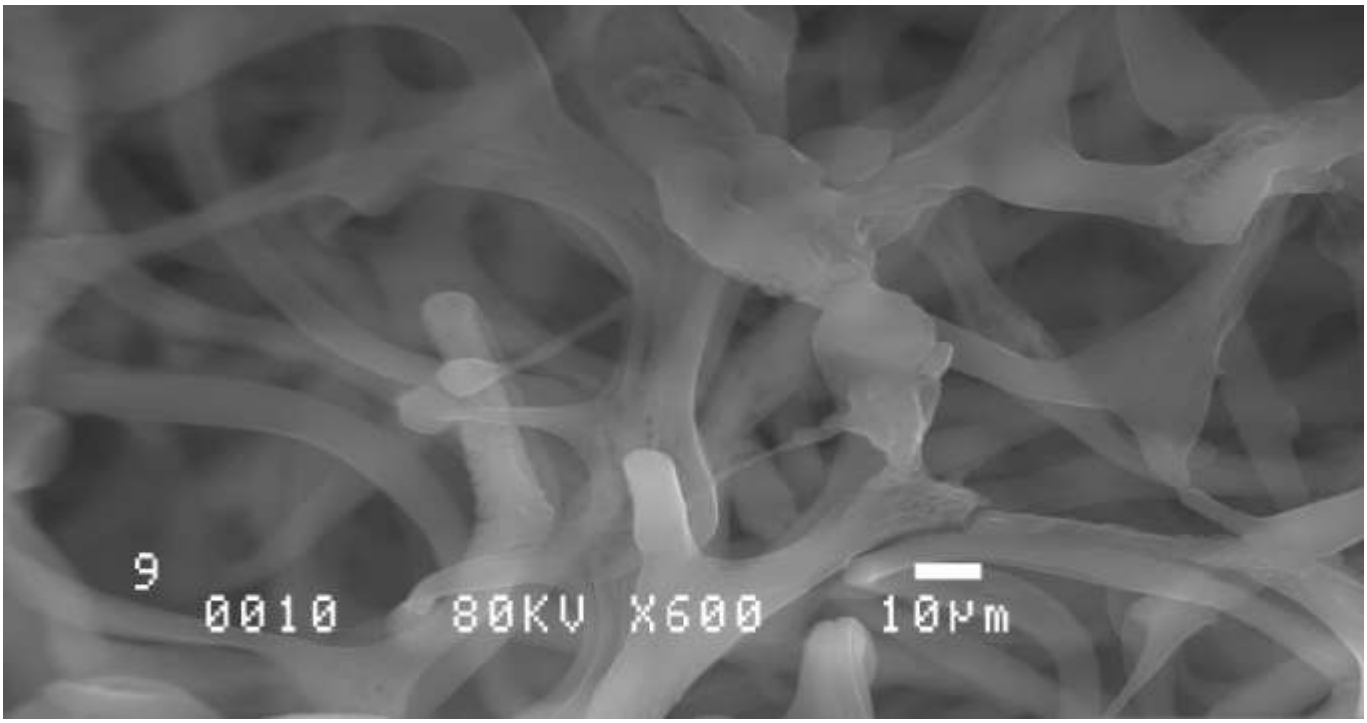

Figure 3.20 SEM Micrograph of silk fibroin scaffold

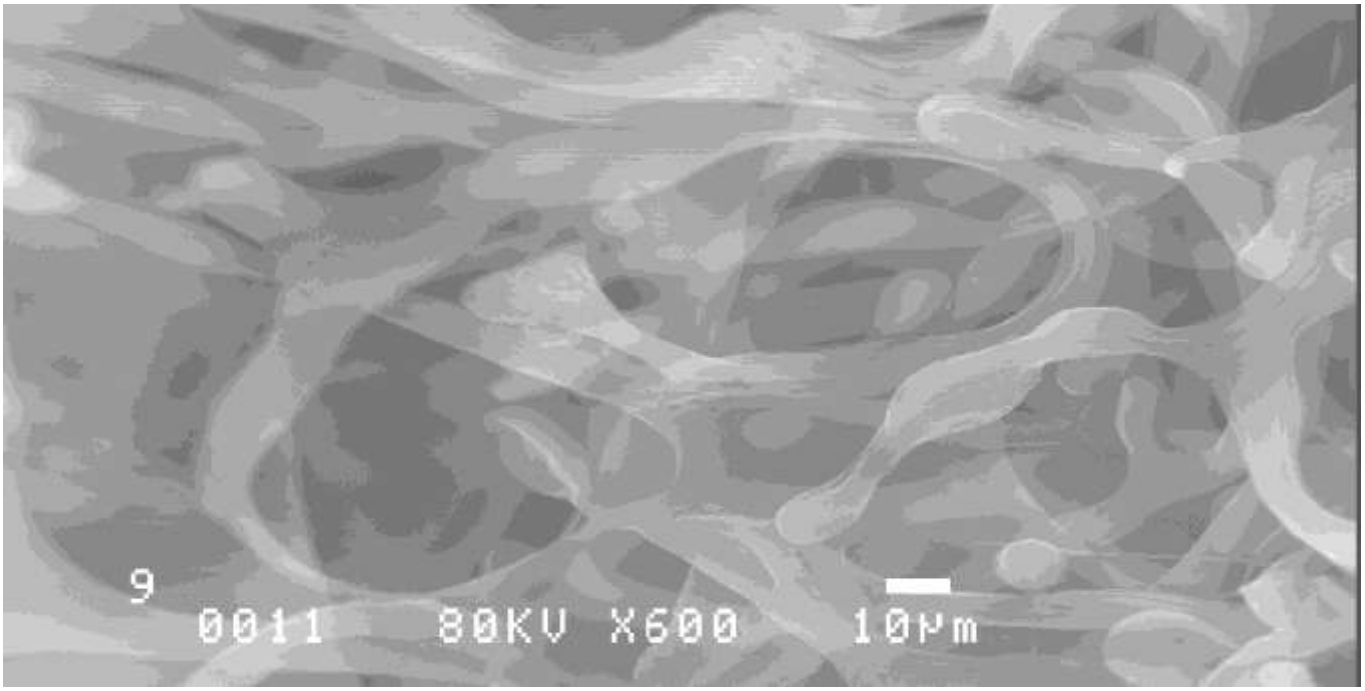

Figure 3.21 SEM Micrograph of silk fibroin scaffold

These two SEM Micrographs of the same scaffold shown in Figure 3.20 and Figure 3.21 shows, the scaffold's porous and non-porous regions and it shows that it is suitable for cell culturing for the cells can integrate within the scaffold to form a tissue as well as embedding growth factors or drugs. It also shows that the pore sizes are very large if the scaffold is prepared at -80°C this indicates that the swelling of the scaffolds either in PBS or in ABS are higher than the ones prepared at -20°C.

3.4 Activated partial thromboplastin time (APTT),Prothrombin time (PT) and International normalized ratio (INR).

Table.12 The Normal Clot Time DATA ranges for Healthy Persons.

APTT	PT(Sec)	PT (%)	INR
23.6-35.2	11.5-15	70%-120%	0.8-1.2

Table.13 Data of the test Plasma Sample (from healthy person)

APTT	PT(Sec)	PT (%)	INR
29.3	13	107%	0.96

Table.14 *In Vitro* Clot Time of Prothrombin Time (PT), the Activated Partial Thromboplastin Time (APTT), INR.

Sample	ΔT(minute)	PT	INR	PT(Sec)	APTT(Sec)
A1	5 min	30%	2.48	26.8	90.3
	5min	30%	2.47	26.7	91.3
	10 min	26%	2.89	30.1	94
	10 min	26%	2.90	30.8	96.1
A2	5 min	29%	2.55	27.4	93.9
	5 min	29%	2.54	27.3	93.2
	10 min	26%	2.84	29.7	95.5
	10 min	26%	2.86	29.9	94.6

The *in vitro* anticoagulant activities of the silk fibroin scaffolds were evaluated by activated partial thromboplastin time (APTT), and prothrombin time (PT) measurements. The results showed that both silk fibroin scaffolds prepared at -80°C and -20°C exhibited good biocompatibility properties. The swelling property of the scaffold in the plasma was also evaluated and swelling ratio was calculated as 96.8%.

3.5 X-Ray Diffraction (XRD) Analysis

X-Ray diffraction of raw silk fibroin gives three characteristic crystallinity peaks at 2θ=11.62°, 20.56° and 10.46°. In the crosslinked sample new weaker crystalline peaks appear at 12.58°, 20.50° and 9.12°. The silk fibroin scaffold gives 3 characteristic crystallinity at 2θ=20.42°, 19.48° and 21.18°. So both the crystalline structure and the degree of crystallinity are affected as a result of crosslinking and freeze drying. The data and the results are summarized in Table.15. The percent crystallinity for the samples SFS used in the scaffold has been calculated as the SFX sample is completely amorphous.

Table.15 X-Ray Diffraction Analysis of Silk Fibroin and Silk Fibroin Scaffold Prepared by Freeze Drying Technique at -80°C.

Sample	Strongest peak no.	2 Theta (deg)	$d_{(A)}$	I/I1	FWHM(deg)	Intensity(counts)	Integrated Int.(counts)
SF (raw silk fibroin)	6	11.6200	7.60940	100	2.24000	37	3290
	11	20.5600	4.31640	76	2.10000	28	2493
	5	10.4600	8.45053	68	1.20000	25	1099
SFX(silk fibroin film)	7	12.5800	7.03080	100	1.16000	17	1577
	15	20.5000	4.32890	100	1.40000	17	1133
	4	9.1200	9.68894	94	1.04000	16	1003
SFS (silk fibroin scaffolds)	16	20.4200	4.34568	100	0.00000	111	0
	15	19.4800	4.55321	86	0.00000	95	0
	17	21.1800	4.19143	86	0.00000	95	0

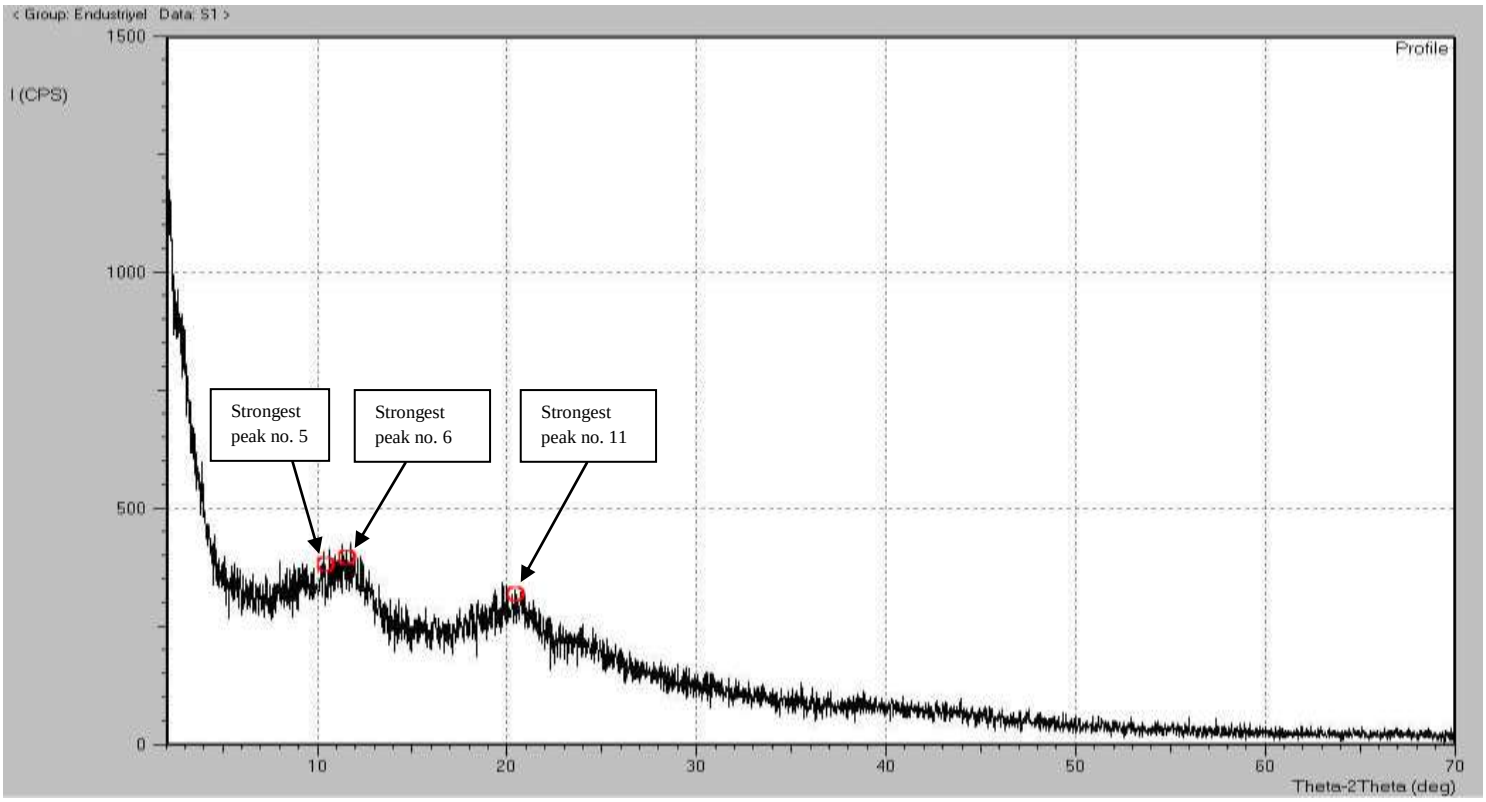

Figure 3.22 XRD pattern of silk fibroin

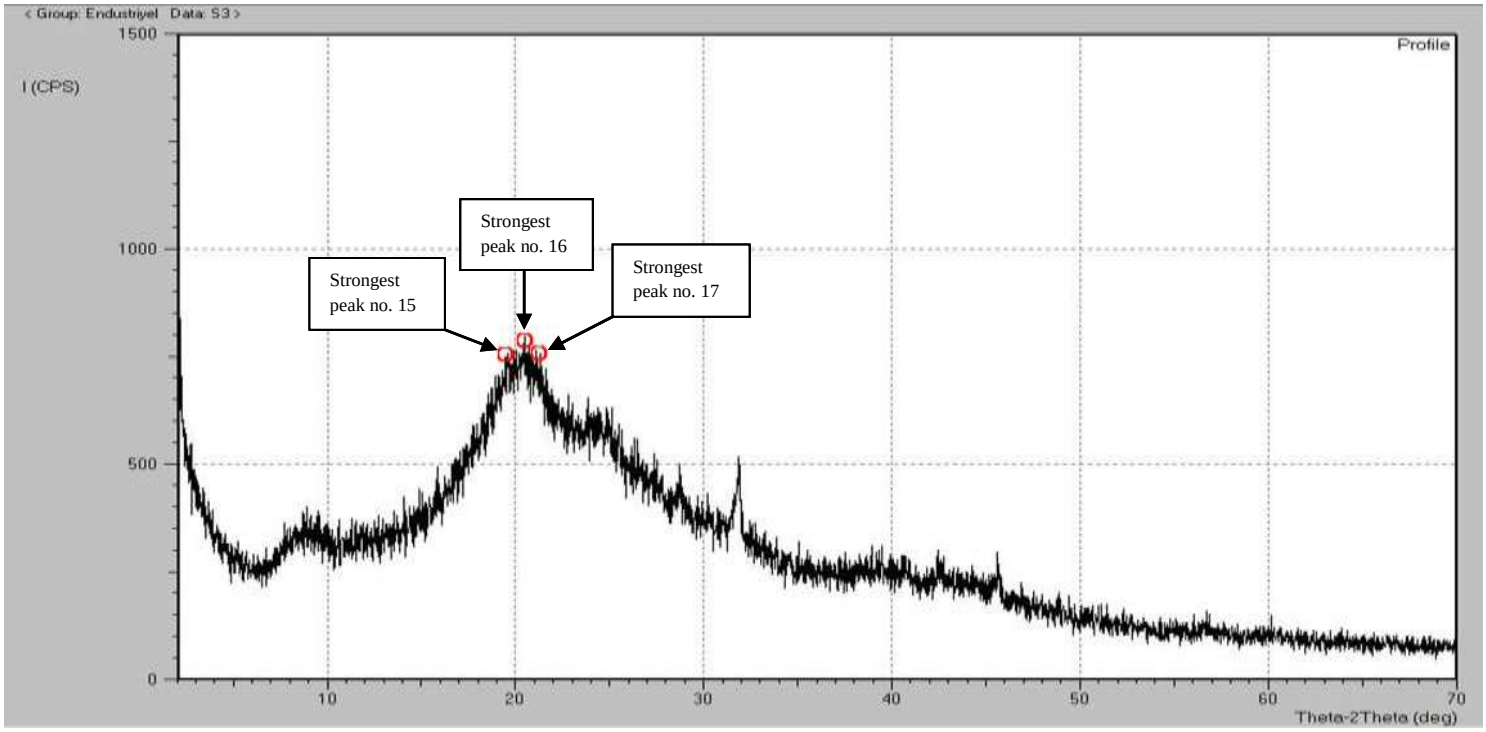

Figure 3.23 XRD pattern of silk scaffold prepared by freeze drying at -80°C

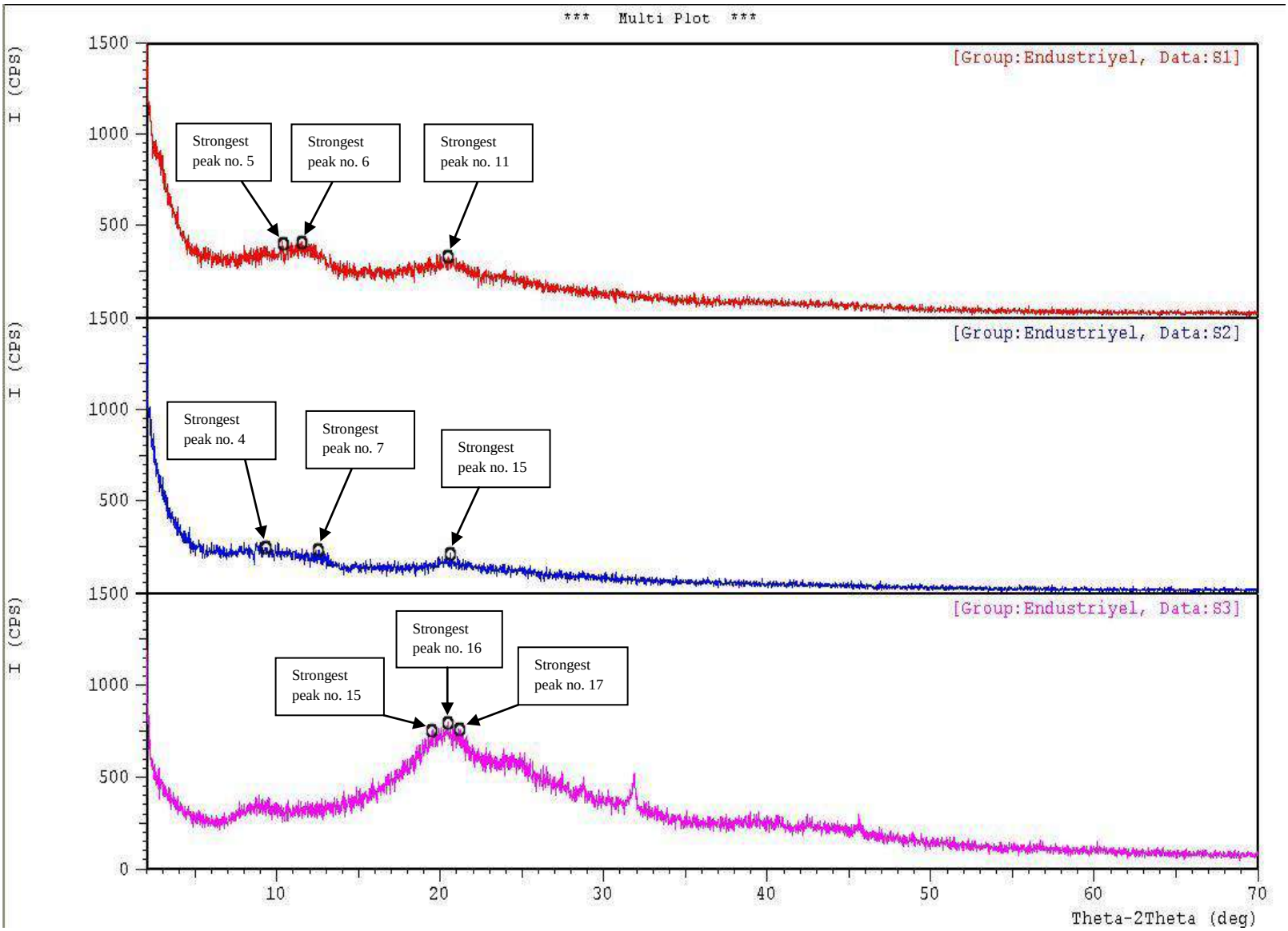

Figure 3.24 Comparison of (a) raw silk fibroin XRD pattern (b) silk fibroin film with prepared by UV induced photopolymerization technique under homogeneous conditions. (c) XRD pattern of silk fibroin scaffold prepared by freeze drying technique at -20°C.

3.6 Discussions and Conclusions

Various forms of silk fibroin scaffolds were prepared by freeze drying technique at -20C and -80^{o}C. The effects of temperature, swelling ratio (weight %), crosslinker concentration were examined on the physicochemical properties of the scaffolds. Silk fibroin scaffolds are susceptible to enzymatic degradation upon treatment with protease enzyme as an indication of biodegradability. All silk fibroin scaffolds were water and acid insoluble. They sampled both in sodium hydroxide and acidic solution. Increasing the methylene bisacrylamide $C_7H_{10}N_2O_2$ concentration in the reaction medium induced crosslinking reactions. Products were either partially or highly crosslinked and hence produced insoluble products.

The SEM analysis showed:

(i) The effectiveness of the degumming process as it removed the sericin from the silk fibers which is observed by the smoothness of the fiber's surface and the absence of the sericin protein.

(ii) The SEM micrographs of the films showed the role of the crosslinker in smoothing the surface.

(iii) The SEM micrograph of the silk fibroin scaffold prepared at -80°C revealed the porous structure of the scaffold which can be utilized as perfect home for the cell due to its porosity, biocompatibility and its ability to hold different growth factors and drugs.

According to XRD analysis;

(i) Both the crystalline structure and the degree of crystallinity of silk fibroin and affected as a result of structural formation processes.

(ii) As the silk fibroin forms films (thinner scaffolds) %crystallinity of the scaffolds increases.

(iii) The presence of the crosslinker in the scaffold aids the formation of ordered structure.

The scaffolds swelling exhibited a high pH sensitivity .these scaffolds may be considered as an excellent candidate to design targetable drug delivery systems. The *in vitro* coagulation time tests have been applied and results showed that prothrombin time and APTT were prolonged by mixing the plasma with silk fibroin scaffold. This indicates that, the final products are ideal candidates for blood compatible biomedical applications.

References

[1] J. Perez-Rigueiro, M.E., J. Llorca, C. Viney, "Tensile Properties of Silkworm Silk Obtained by Forced Silking", *Journal of Applied Polymer Sciences*,2001.**82**: p. 1928-1935.

[2]Haifeng Liu, Z.G., Yue Wang, SiewLokToh, VallayaSutthikkum, James C.H. Goh, "Modification of sericin-free silk fibers for ligament tissueengineering application", *Journal of Biomedical Materials Research Part B: Applied Biomaterials*, 2006. **10**: p. 129-138.

[3] Tatyana Dyakonov, Chue Hue Yang, Derek Bush, SaujanyaGosangari, ShingaiMajuru, and AqeelFatmi "Design and Characterization of A Silk-Fibroin-Based Drug Delivery Platform using Naproxen as a model Drug", *Journal of Drug Delivery* Volume 2012, Article ID 490514, 10 pages doi:10.1155/2012/490514.

[4] Valluzzi, Regina; Gido, Samuel P.; Muller, Wayne; Kaplan, David L. "Orientation of Silk III At The Air-Water Interface". *International Journal of Biological Macromolecules* 24 (2-3) (1999) 237–242.

[5]ShaileshNagarkar, A.P., AshishLele, Suresh Bhat, JayeshBellare, R.A. Mashelkar, "Some Mechanistic Insights Into The Gelation of Regenerated Silk fibroin Sol.", *Industrial and Engineering Chemistry Research*, 2009. **48**(17): p. 8014-8023.

[6]ShaileshNagarkar, T.N., Christophe Chassenieux, AshishLele, "Structure and Gelation Mechanism of Silk Hydrogels", *Physical Chemistry ChemicalPhysics*, 2010.**12**: p. 3834-3844.

[7]Qiang Zhang, S.Y., Mingshong Li, "Silk Fibroin Based Porous Materials". *Materials*, 2009.**2**: p. 2276-2295.

[8] Jin, Hyoung-Joon, and David L. Kaplan. "Mechanism of silk processing in insects and spiders", *Nature* 424, no. 6952 (2003): 1057-1061.

[9] Gregory H. Altman, F.D., Caroline Jakuba, Tara Calabro, Rebecca L. Horan, Jingsong Chen, Helen Lu, John Richmond, David L. Kaplan, "Silk Based Biomaterials". *Biomaterials*, 2003.**24**: p. 401-416.

[10] A. Alessandrino, B.M., C. Arosio, S. Fare, M.C. Tanzi, G. Freddi, "Electrospun Silk Fibroin Mats For Tissue Engineering". *Engineering Life Science*, 2008.**8**(3): p. 219-225.

[11] V. Kearns, A.C.M., A. Crawford, P.V. Hatton, "Silk-Based Biomaterials For Tissue Engineering", *in Topics in Tissue Engineering*, Vol. 4. Eds. N Ashammakhi, R Reis, & F Chiellini 2008. p. 1-19.

[12] OguzBayraktar, O.M., YarkinOzgarip, AysegulBatigun, "Silk Fibroin As A Novel Coating Material For Controlled Release Of Theophylline". *European Journal of Pharmaceutics and Biopharmaceutics*, 2005.**60**: p. 373-381.

[13] Lin Liu, J.L., Mingqi Wang, Sinjia Min, YurongCai, Liangjun Zhu, JumingYao,"Preparation And Characterization Of Nano-Hydroxyapatite/Silk Fibroin Porous Scaffolds". *Journal of Biomaterials Science Polymer Edition*, 2008.**19**(3): p. 325-338.

[14] Simone S. Silva, D.M., Antonella Motta, Joao F. Mano, Rui L. Reis, Claudio Migliaresi, "Genipin-Modified Silk-Fibroin Nanometric Nets*".Macromolecular Bioscience*, 2008.**8**(8): p. 766-774.

[15] Hyoung-Joon Jin & David L. Kaplan, "Mechanism of silk processing in insects and spiders", *Nature* 424, (28 August 2003) 1057-1061.

[16] Lim Jeong, K.Y.L., Won Ho Park, "Effect Of Solvent On The Characteristics Of Electrospun Regenerated Silk Fibroin Nanofibers". *Key Engineering Materials*, 2007.**342**: p. 813-816.

[17] Mao Wang, H.-J.J., David L. Kaplan, Gregory C. Rutledge, "Mechanical Properties Of Electrospun Silk Fibers". *Macromolecules*, 2004.**37**: p. 6856-6864.

[18] Yongzhong Wang, D.D.R., Ashley Walsh, Lauren Abrahamsen, Hyeon-Joo Kim, Hyun S. Kim, Carl Kirker-Head, David L. Kaplan, "*In vivo* degradation of three-dimensional silk fibroin scaffolds". *Biomaterials*, 2008.**29**: p. 3415-3428.

[19] H. Ueda, L.H., M. Yamamoto, K. Shigeno, M. Inoue, T. Toba, et al., "Use of collagen sponge incorporating transforming growth factor-beta 1 to promote bone repair in skull defects in rabbits". *Biomaterials*, 2002.**23**(4): p. 1003-1010.

[20] H. Sun, L.M., C. Song, X. Cui, P. Wang, "The *in vivo* degradation, absorption and excretion of PCL-based implant".*Biomaterials*, 2006.**27**(9):p. 1735-1740.

[21] M. Ramchandani, M.P., D. Robinson, "The influence of manufacturing procedure on the degradation of poly(lactide-co-glycolide) 85:15 and 50:50 implants". *Journal of.Controlled Release*, 1997.**43**(2-3): p. 161-173.

[22] G. Kister, G.C., M. Vert, "Structure and morphology of solid lactide-glycolide copolymers from C-13 nmr, infra-red and Raman Spectroscopy*".Polymer*, 1998. **39**(15): p. 3335-3340.

[23] S. Liao, F.W., Y. Zhu, M. Uo, T. Akasaka, W. Wang, et al., "The degradation of the three layered nano-carbonated hydroxyapatite/collagen/PLGA composite membrane *in vitro*". *Dent Mater*,2007. **23**(9): p. 1120-1128.

[24] NA Peppas, AR. Khare, "Preparation, Structure and Diffusional Behavior of Hydrogels in Controlled Release", *Advanced Drug Delivery Reviews*. 11(1993)1—35.

[25] M. Haider, V. Leung. F. Ferran j. Crissman,j. Powell, j. Cappello, H. Ghandeharj, "Molecular Engineering Of Silk-Elastinlike Polymers For Matrix-Mediated Gene Delivery: Biosynthesis And Characterization", *Molecular Pharmaceutics.*2 (2) (2005) 139—150.

[26]. Rujiravanit S. Kruaykitanon A.M. Jamieson, S. Tokura, "Preparation of Crosslinked Chitosan/Silk Fibroin Blend Films for Drug Delivery System", *Macromolecular Bioscience.* 3 (2003) 604—611.

[27] AS. Gobin, V.E. Froude, A.B. Mathur, "Structural And Mechanical Characteristics of Silk Fibroin and Chitosan Blend Scaffolds For Tissue Regeneration", *Journal of Biomedical Materials Research* 74 (3) (2005) 465-473.

[28] M. Garcia-Fuentes E. Giger, L Meinel, H.P. Merkie, "The Effect of Hyaluronic Acid on Silk Fibroin Conformation", *Biomaterials* 29 (6) (2008) 633-642.

[29] D.L. Kaplan, C.M. Mello, S. Arcidiacono, S. Fossey, K. Senecal, W. Muller, in: K.McGrath, D.L Kaplan (Eds), "Protein Based Materials", *Birkhauser, Boston*, 1997, pp. 103-131.

[30] D.M Phillps, L.F. Drummy, D.G. Conrady, D.M Fox, R.R Naik, M.O. Stone, P.C. Truelove, H.C. De long, R.A Mantz, "Dissolution and Regeneration of *Bombyx Mori* Silk Fibroin Using Ionic Liquids", *J. Am . Chem .Soc* 126 (44) (2004) 14350-14351.

[31] L Meinel, S. Hofmann. V. Karageorgiou. C Kirker-Head,j. McCooI. G. Gronowicz, L Zichner, R. Langer, G. Vunjak-Novakovic, D.L. Kaplan, "The Inflammatory Responses To Silk Films *In Vitro* And *In Vivo*", *Biomaterials* 26 (2) (2005) 147-155.

[32] L Uebersax. T. Apfel, K.M.R Nuss, R. Vogt, H.Y. Kim, L Meinel, D.L Kaplan, J.A. Auer. H.P. Merkle. B. von Rechenberg, "Silk Fibroin Scaffolding for Growth Factor Delivery in Tissue Repair", Diss. ETh No. 17551. 2008.

[33] Y. Wang, D.D Rudym, A. Walsh, L Abrahamsen H.j. Kim, H.S. Kim, C Kirker-Head, D.L Kaplan, "*In Vivo* Degradation Of Three Dimensional Silk Fibroin Scaffolds", *Biomaterials* 29 (24-25) (2008) 3415—3428.

[34] Motta, Antonella, DevidManiglio, Claudio Migliaresi, Hyeon-Joo Kim, Xianyan Wan, Xiao Hu, and David L. Kaplan. "Silk Fibroin Processing and Thrombogenic Responses." *Journal of Biomaterials Science, Polymer Edition* 20, no. 13 (2009): 1875-1897.

[35] Panilaitis, Bruce, Gregory H. Altman, Jingsong Chen, Hyoung-Joon Jin, VassilisKarageorgiou, and David L. Kaplan. "Macrophage Responses to Silk."*Biomaterials* 24, no. 18 (2003): 3079-3085.

[36] ThanonchatImsombut, YaowalakSrisuwan, PrasongSrihanam, YodthongBaimark, "Genipin-Cross-Linked Silk Fibroin Microspheres Prepared By the Simple Water-In-Oil Emulsion Solvent Diffusion Method", *Powder Technology,* 203 (2010) 603-608.

[37] Joo-Hong Yeo , Kwang-Gill Lee , Yong-Woo Lee , Sun Yeou Kim "Simple Preparation And Characteristics Of Silk Fibroin Microsphere", *European Polymer Journal* 39 (2003) 1195-1199.

[38] Esther Wenk , Anne J. Wandrey , Hans P. Merkle . Lorenz Meinel "Silk Fibroin Spheres As A Platform For Controlled Drug Delivery" / Journal of Controlled Release 132(2008) 26-34.

[39] Seung Jun Myung,Hun-SikKim,YeseulKim,PengChen,andHyoung-Joon,Jin, "Fluorescent Silk Fibroin Nanoparticles Prepared Using A Reverse Microemulsion", *Macromolecular research*,vol. 16,No. 7(2008), pp604-608.

[40] Vishal Gupta , Abraham ,Aseh , Carmen N Rios , Bharat B Aggarwal , Anshu B Mathur "Fabrication And Characterization Of Silk Fibroin-Derived Curcumin Nanoparticles For Cancer Therapy", *International Journal of Nanomedicine*, (2009):4 115-122.

[41] JoydipKundu , Yong-Il Chung , Young Ha Kim , Giyoong Tae , S.C.Kundu "Silk Fibroin Nanoparticles For Cellular Uptake And Control Release" / International Journal of pharmaceutics 388(2010) 242-250.

[42] HaeYongKweon, Joo-Hong Yeo, SoonOk Woo, SangMi Han, You Young Jo and Kwang-Gill Lee "Preparation and Characterization of Silk Fibroin Nanoparticles", *International Journal of Industrial Entomology*,Vol. 20, No. 1, 2010, pp. 25~28.

[43] Chaoyang Jiang, Xianyan Wang, Ray Gunawidjaja, Yen-Hsi Lin, Maneesh K. Gupta, David L. Kaplan, Rajesh R. Naik, Vladimir V. Tsukruk "Mechanical Properties of Robust Ultrathin Silk Fibroin Films". *Advanced Functional Materials*, **2007**, *17*, 2229–2237

[44] JinweiGu, Xinlin YangHesun Zhu "Surface Sulfonation Of Silk Fibroin Film By Plasma Treatment And *In Vitro* Antithrombogenecity Study", *Materials Science and Engineering: C*Volume 20, Issues 1–2, 31 May 2002, Pages 199–202.

[45] VassilisKarageorgiou, Lorenz Meinel, Sandra Hofmann, Ajay Malhotra, Vladimir Volloch, David Kaplan, "Bone Morphogenetic Protein-2 Decorated Silk Fibroin Films Induce Osteogenic Differentiation Of Human Bone Marrow Stromal Cells". *Journal of Biomedical Materials Research Part A* Volume 71A, Issue 3, pages 528–537, 1 December 2004.

[46] Lorenz Uebersaxa, Marta Mattottia, MichaëlPapaloïzosb, Hans P. Merklea, Bruno Gandera, Lorenz Meinela, "Silk fibroin matrices for the controlled release of nerve growth factor (NGF)" *Biomaterials* ,Volume 28, Issue 30, October 2007, Pages 4449–4460.

[47]. W E Teo, S.R., "A Review on Electrospinnig Design and Nanofiber Assemblies". *Nanotechnology*, 2006.**17**: p. R89-R106.

[48]. A. Alessandrino, B.M., C. Arosio, S. Fare, M.C. Tanzi, G. Freddi, "Electrospun Silk Fibroin Mats For Tissue Engineering". *Engineering Life Science*, 2008.**8**(3): p. 219-225.

[49]. Wan-Ju Li, R.M.S., Rocky S Tuan, "Electrospinning Technology for Nanofibrous Scaffolds in Tissue Engineering, In Tissue", *cell and organ engineering*, C. Kumar, Editor. 2006, Wiley-VCH: Weinheim. p. 135-180.

[50]. Sachiko Sukigara, M.G., Jonathan Ayutesede, Michael Micklus, Frank Ko, “Regeneration Of *Bombyx Mori* Silk By Electrospinning - Part 1: Processing Parameters And Geometric Properties.” *Polymer*, 2003.**44**: p. 5721-5727.

[51]. CharuVepari, D.L.K., “Silk as a Biomaterial.” *Progress in Polymer Science*, 2007.**32**: p. 991-1007.

[52] RupeshNawalakhe a, Quan Shi a, NarendiranVitchuli a, Mohamed A. Bourham, Xiangwu Zhang, Marian G. McCord, “Novel Atmospheric Plasma Enhanced Silk Fibroin Nanofiber/Gauze Composite Wound Dressings” *Journal of Fiber Bioengineering & Informatics* 5:3 (2012) 227-242

[53]. ShaileshNagarkar, A.P., AshishLele, Suresh Bhat, JayeshBellare, R.A. Mashelkar, “Some Mechanistic Insights into the Gelation of Regenerated Silk Fibroin Sol.” *Industrial and Engineering Chemistry Research*, 2009.**48**(17):p. 8014-8023.

[54]. Yuji Miyaguchi, J.H., “Physicochemical Properties of Silk Fibroin After Solubilization Using Calcium Chloride With or Without Ethanol”. *Food Science and Technology Research*, 2005.**11**(1): p. 37-42.

[55]. Xiaoqin Wang, J.K., Gary G. Leisk, David L. Kaplan, “Sonication-Induced Gelation of Silk Fibroin For Cell Encapsulation.” *Biomaterials*, 2008.**29**(8): p.1054-1064.

[56]. M.A. Moraes, M.F.S., G.M. Nogueira, M.M. Beppu. “Silk Fibroin Hydrogels Formed By Addition of Ethanol.” *in 11th International Conference on Advanced Materials*. 2009. Rio de Janeiro, Brazil.

[57]. Tamada, Y., “New Process To Form A Silk Fibroin Porous 3-D Structure.” *Biomacromolecules*, 2005.**6**(6): p. 3100-3106.

[58]. RinaNazarov, H.-J.J., David L. Kaplan, “Porous 3-D Scaffolds From Regenerated Silk Fibroin.” *Biomacromolecules*, 2004.**5**: p. 718-726.

[59]. Ung-Jin Kim, J.P., Chunmei Li, Hyoung-Joon Jin, Regina Valluzzi, David L. Kaplan, “Structure and Properties of Silk Hydrogel.” *Biomacromolecules*, 2004.**5**: p. 786-792.

[60] Gregory H. Altmana, Rebecca L. Horana, Helen H. Lua, Jodie Moreaua, Ivan Martinb, John C. Richmondc, David L. Kaplana, "Silk Matrix For Tissue Engineered Anterior Cruciate Ligaments," *Biomaterials*, 23 (2002), 4131–4141.

[61] Benjamin Dararutana, SittisakHonsawek, SiripornDamrongsakkul, “Characterization of Thai Silk Fibroin/Gelatin Based Scaffolds Incorporated With Hydroxiapatite and **β**-Tricalcium Phosphate”

[62] Lin Niu, RuiZou, Qida Liu, Quanli Li, Xinmin Chen, and Zhiqing Chen “A Novel Nanocomposite Particle of Hydroxyapatite and Silk Fibroin: Biomimetic Synthesis and Its Biocompatibility” *Journal of Nanomaterials* Volume 2010, Article ID 729457, 7 pages.

[63] Le-Ping Yan , Joaquim M. Oliveira , Ana L. Oliveira , Sofia G. Caridade , João F. Mano , Rui L. Reis , " Macro/Microporous Silk Fibroin Scaffolds With Potential For Articular Cartilage And Meniscus Tissue Engineering Applications," *ActaBiomaterialia*, xxx (2011) xxx–xxx.

[64] Hua-Xiao Yang,Min Sun, Yi Zhang, and Ping Zhou, “Degradable PHBHHxModified by the Silk Fibroin for the Applications of Cardiovascular Tissue Engineering”, *ISRN Materials Science* Volume 2011, Article ID 389872, 11 pages doi:10.5402/2011/389872.

[65] Yumin Yang1, Xuemei Chen1, Fei Ding, Peiyun Zhang, Jie Liu, XiaosongGu, “Biocompatibility Evaluation Of Silk Fibroin With Peripheral Nerve Tissues And Cells *In Vitro* ”, *Biomaterials* 28 (2007) 1643–1652.

[66] BorisutSanmano Hanpanich1_, Bovornlak Oonkhanond2, Vichai Srimuninnimit2, Vivat Visuthikosol3, and Prasert Sophon4 “De Novo Method Of Developing Silk Fibroin Hydrogel Aim For Using As A Dermal Scaffold By Gamma Irradiation.”

[67] AndreiaVasconcelos, Andreia C. Gomes, ArturCavaco-Paulo, "Novel Silk Fibroin/Elastin Wound Dressings," *ActaBiomaterialia*, 8 (2012), 3049–3060.

[68] Yongpei Hu, Qin Zhang, Renchuan You, LingshuangWang, andMingzhong Li, “The Relationship between Secondary Structure and Biodegradation Behavior of Silk Fibroin Scaffolds” *Advances in Materials Science and Engineering* Volume 2012, Article ID 185905, 5 pages doi:10.1155/2012/185905

[69] M. K. Sah and K. Pramanik, "Regenerated Silk Fibroin From B. Mori Silk Cocoon For Tissue Engineering Applications," *International Journal of Environmental Science and Development,* Vol.1, No.5, December (2010), ISSN: 2010-0264.

[70] Cho Se Youn, Heo Semi, Jin Hyoung-Joon "Controlling Microstructure Of Three-Dimensional Scaffolds From Regenerated Silk Fibroin By Adjusting Ph". *J NanosciNanotechnol*. 2012 Jan; 12(1):806-10.

[71] Zhang Yufeng, Fan Wei, Ma Zhaocheng, Wu Chengtie, Fang Wei, Liu Gang, Xiao Yin. "The Effects of Pore Architecture in Silk Fibroin Scaffolds on the Growth and Differentiation of Mesenchymal Stem Cells Expressing Bmp7".*ActaBiomater*. 2010 Aug; 6(8):3021-8.

[72] Garcia-Fuentes M, Meinel AJ, Hilbe M, Meinel L, Merkle HP. "Silk Fibroin/Hyaluronan Scaffolds For Human Mesenchymal Stem Cell Culture In Tissue Engineering". *Biomaterials*, 2009 Oct; 30(28):5068-76.

[73] Cristina Correia, SarindrBhumiratana, Yan Leping, Ana L. Oliveira, Jeffrey M. Gimble, David L. Kaplan, Rui A. Sousa, GordanaVunjak-Novakovic, Rui L. Reis."The Influence of Silk Fibroin 3d Scaffold Composition for *In Vitro* Bone Tissue Engineering" *Bone* 70: 90.

[74] Hyoung-Joon Jin, Jingsong Chen, VassilisKarageorgiou, Gregory H. Altman, David L. Kaplan "Human Bone Marrow Stromal Cell Responses on Electrospun Silk Fibroin Mats", *Biomaterials* 25 (2004) 1039–1047.

[75] Fre´de´ricByette , Fre´de´ric Bouchard , Christian Pellerin , Joanne Paquin , Isabelle Marcotte , Mircea A. Mateescu, "Cell-Culture Compatible Silk Fibroin Scaffolds Concomitantly Patterned By Freezing Conditions and Salt Concentration", *Polymer Bulletin*, (2011) 67:159–175.

[76] Yufeng Zhang, Wei Fan, Zhaocheng Ma, Chengtie Wu, Wei Fang, Yin Xiao "The Effects of Pore Architecture in Silk Fibroin Scaffolds on The Growth and Differentiation of Mesenchymal Stem Cells Expressing BMP7", *ActaBiomaterialia*, (2010) 6(8). pp.3021-3028.

[77] SedaTığlı, R., SourabhGhosh, Michael M. Laha, Nirupama K. Shevde, Laurence Daheron, Jeffrey Gimble, MenemşeGümüşderelioğlu, and David L. Kaplan. "Comparative chondrogenesis of human cell sources in 3D scaffolds." *Journal of tissue engineering and regenerative medicine* 3, no. 5 (2009): 348-360.

[78] Sandra Hofmann, Henri Hagenmuller, Annette M Koch, Ralph Muller, Gordana, Vunjak-Novakovic, David L Kaplan, Hans P Merkle, Lorenz Meinel. “Control of *in vitro* tissue-engineered bone-like structures using human mesenchymal stem cells and porous silk scaffolds”.*Biomaterials*. 2007 Feb; 28(6):1152-62.

[79] Meinel, Lorenz, VassilisKarageorgiou, Robert Fajardo, Brian Snyder, VivekShinde-Patil, Ludwig Zichner, David Kaplan, Robert Langer, and GordanaVunjak-Novakovic. "Bone Tissue Engineering Using Human Mesenchymal Stem Cells: Effects of Scaffold Material and Medium Flow." *Annals of biomedical engineering* 32, no. 1 (2004): 112-122.

[80] Hofmann, Sandra, Sven Knecht, Robert Langer, David L. Kaplan, GordanaVunjak-Novakovic, Hans P. Merkle, and Lorenz Meinel. "Cartilage-Like Tissue Engineering Using Silk Scaffolds and Mesenchymal Stem Cells."*Tissue engineering* 12, no. 10 (2006): 2729-2738.

[81] Schmaier AH. Laboratory evaluation of hemostatic and thrombotic disorders. In: Hoffman R, Benz EJ Jr., Shattil SJ, et al, eds. *Hoffman Hematology: Basic Principles and Practice*. 5th ed. Philadelphia, Pa: Churchill Livingstone Elsevier; 2008: chap 122.

[82] Wolfgang Korte, MD, Susan Clarke, MT(ASCP), and Jerry B. Lefkowitz, MD. "Short Activated Partial Thromboplastin Times Are Related to Increased Thrombin Generation and an Increased Risk for Thromboembolism". *Am J ClinPathol.* (2000) (113): 123–127.

[83] GrahamColm, “The components and pathways that make up the classical blood coagulation cascade”,*https://commons.wikimedia.org/wiki/File:Classical_blood_coagulation_pathway.png*(15 April 2012)

[84] Fritsma, George A. "Evaluation of Hemostasis." *Hematology: Clinical Principles and Applications . Ed. Bernadette Rodak. W.B. Saunders Company*: Philadelphia, 2002. 719-53. Print

[85] Freyburger G, Labrouche S. “Comparabilty of D-dimer assays in clinical samples.” *Seminars in Vasc Medicine* 2005;5:328-339.

[86] Ansell J, Hirsh J, Poller L, et al: The pharmacology and management of the vitamin K antagonists. Chest 2004; 126 (Suppl 3):204S-233S.

[87] Salem DN, Stein PD, Al-Ahmed A, et al: Antithrombotic therapy in valvular heart disease - native and prosthetic: the seventh ACCP conference on antithrombotic and thrombolytic therapy. Chest 2004; 126:457S-482S.

[88] Buller HR, Agnelli G, Hull RD, et al: Antithrombotic therapy for venous thromboembolic disease: the Seventh ACCP Conference on Antithrombotic and Thrombolytic Therapy. Chest 2004; 126(3 Suppl)::401S-428S.

[89] Ansell J, Hirsh J, Dalen J, et al: Managing oral anticoagulant therapy.. Chest 2001; 119(1 Suppl):22S-38S.

[90] Henry JB: Clinical Diagnosis and Management by Laboratory Methods, 20th ed. Saunders, 2001.

[91] Nicoll D, McPhee SJ, Pignone M, et al (Eds): Pocket Guide to Diagnostic Tests, 3rd. McGraw-Hill, New York, NY, United States, 2001.

[92] Riley RS, Rowe D, & Fisher LM: Clinical utilization of the international normalized ratio (INR). J Clin Lab Anal 2000; 14(3):101-14.

[93] Haemostatis and Thrombosis Task Force of the British Society for Standards in Haematology: Guidelines on oral anticoagulation: third edition. Br J Haematol 1998; 101(2):374-287.

[94] Tietz NW (Ed): Clinical Guide to Laboratory Tests, 3rd ed. W. B. Saunders, Philadelphia, PA, 1995.

[95] Jaworska, Malgorzata, Kensuke Sakurai, Pierre Gaudon, and Eric Guibal. "Influence of chitosan characteristics on polymer properties. I: Crystallographic properties." *Polymer international* 52, no. 2 (2003): 198-205.

[96] Sahoo, Sambit, SiewLokToh, and James CH Goh. "A bFGF-releasing silk/PLGA-based biohybrid scaffold for ligament/tendon tissue engineering using mesenchymal progenitor cells."*Biomaterials* 31, no. 11 (2010): 2990-2998.

Safwan Mohammad Ali: Non-Thrombogenic Silk Fibroin Scaffolds

Approval of the Director of Graduate School of
Applied Science

Prof. Dr. İlkay SALİHOĞLU

We Certify This Thesis is Satisfactory for the Award of the Degree of Master of Science in Biomedical Engineering.

Examining Committee in charge:

Prof. Dr. İlkay SALİHOĞLU	**Committee Chairman, Biomedical Engineering Department, NEU.**
Prof. Dr. Nedime SERAKINCI	**Committee Member, Medical Genetics Department, NEU.**
Assist. Prof. Dr. Umut Fahrioğlu	**Committee Member, Medical Genetics Department, NEU.**
Assist. Prof. Dr. Terin ADALI	**Committee Member (Supervisor), Biomedical Engineering Department, NEU.**
Assist. Prof. Dudu ÖZKUM	

DECLARATION

I hereby declare that this thesis is my own work and effort and that it has not been submitted anywhere for any award. Where other sources of information have been used, they have been acknowledged.

Signature:

Date:

ABSTRACT

The aim of this study is to modify the blood compatibility property of the silk fibroin scaffolds, the silk fibroin scaffolds were modified by crosslinking N,N'-methylene-di-acrylamide crossliner with freeze drying technique at two different temperature (-20°C and -80°C). Swelling, solubility, morphology, microstructure, chemial composition and crystallinity of the silk fibroin scaffolds were characterized to evaluate the effect of modification by means of scanning electron microscopy (SEM) and X-ray diffraction (XRD).

The results showed that, the swelling percentage of scaffolds prepared at -20°C were less than both in pH = 7.4 and pH = 1.2 than the swelling percentage of the scaffolds prepared at -80°C. The pore sizes of scaffolds prepared at -80^{o}C were greater as the pore sizes of the scaffolds prepared at freezing temperature -20^{o}C. The biodegradation experiments with protease enzyme were tested. The optimum parameters of freezing temperature, crosslinker ratio were also evaluated. The prothrombin time of silk fibroin was very high. The results indicate that the silk fibroin scaffolds could be considered as ideal candidates for tissue engineering applications.

Keywords: Scaffolds, Silk fibroin, Blood compatible Biomaterial, Prothrombin time (PT), N,N'-methylene-di-acrylamide

ÖZET

Bu çalışmada, lypofil tekniği ile -20^{o}C ve -80^{o}C'de N, N'-metilen dimetakrilamid çapraz bağlayıcısı ile ipek fibroin/ N, N'-metilen dimetakrilamid (SF / N, N'-metilen dimetakrilamid) yapı iskeleleri modifiye edilmiştir. Şişme, çözünme, morfoloji, Kristal yapı, ve kimyasal karışım oranları, Taramalı Elektron Mikroskopu (SEM) ve X-ışın difraksiyonu yöntemi ile değerlendirilmiştir.

Sonuçlar, -20^{o}C'de hazırlanan SF/ N, N'-metilen dimetakrilamid yapı iskelelerinin yüzde şişme miktarının hem fosfat tampon çözelti hem de asit tampon çözeltisinde -80^{o}C'de hazırlanan yapı iskelelerinden daha az olduğu tespit edildi. Donma sıcaklığı, ipek Fibroin / N, N'-metilen dimetakrilamid ağırlık oranları, ve donma süresi optimum değerleri tespit edildi. Proteaz enzimi ile biyobozunur olduğu çalışmalarla ıspatlandı. Protrombin zamanının sınırlar içerisinde yüksek değerlere sahip olduğu gözlemlendi. Elde edilen ürünün kan uyumluluğunun yüksek olduğu belirlendi. Tüm bu sonuçlar, ipek fibroin / N, N'-metilen dimetakrilamid yapı iskelelerinin doku mühendisliği uygulamalarında ideal adaylar arasında söz edilebileceğini göstermiştir.

Anahtar Kelimeler: Yapı iskeleleri, Protrombin Zamanı, İpek Fibroin, Kan uyumlu biyomateryaller, N, N'-metilen dimetakrilamid

ACKNOWLEDGEMENTS

My parents thank you very much for supporting me and having faith in me all this time and thank you for showering me with your love and kindness.

My supervisor, thank you for helping me out in tough spots and having such faith and patience all this time, you were a constant source of support and inspiration.

My family you are the roots of what I am today if am good thank you for whatever you did for me if I'm not then I am sorry for letting you down I should have tried harder following your path.

For my friends and colleagues I hope you succeed through your lives thank you for supporting me.

CONTENTS

LIST OF TABLES

LIST OF FIGURES

LIST OF ABBREVIATIONS

SF	Silk Fibroin
Gly	Glycine
Ala	Alanine
Ser	Serine
n	Number of sequence repetition
PBS	Phosphate Buffer Saline Solution pH 7.4
ABS	Acetic Buffer Solution pH 1.2
Sf80	Scaffold sample prepared at-80°C without any crosslinker
Sf8050	Scaffold sample prepared at -80°C with low crosslinker amount
Sf80300	Scaffold sample prepared at -80°C with high crosslinker amount
Sf20	Scaffold sample prepared at-20°C without any crosslinker
Sf2050	Scaffold sample prepared at -20°C with low crosslinker amount
Sf20300	Scaffold sample prepared at -20°C with high crosslinker amount
R_{se}	Swelling equilibrium ratio
PT	Prothrombin time
APTT	Activated partial thromboplastin time
INR	International normalized ratio (INR)
SEM	Scanning Electron Microscope
XRD	X-Ray Diffraction